10-1-2005

Field Study of the SR 1045 Hares Hill Road Bridge over French Creek in Chester County, PA

Hussam N. Mahmoud

Robert J. Connor

Field Study of the SR 1045 Hares Hill Road Bridge over French Creek in Chester County, Pennsylvania

Final Report

by

Hussam N. Mahmoud

Robert J. Connor

ATLSS Report No. 05-21

October 2005

ATLSS is a National Center for Engineering Research on Advanced Technology for Large Structural Systems

117 ATLSS Drive
Bethlehem, PA 18015-4729

Phone: (610)758-3525
Fax: (610)758-5902

www.atlss.lehigh.edu
Email: inatl@lehigh.edu

Field Study of the SR 1045 Hares Hill Road Bridge over French Creek in Chester County, Pennsylvania

Final Report

by

Hussam N. Mahmoud
Research Engineer
ATLSS Engineering Research Center

Robert J. Connor
Assistant Professor
School of Civil Engineering
Purdue University

ATLSS Report No. 05-21

October 2005

ATLSS is a National Center for Engineering Research on Advanced Technology for Large Structural Systems

117 ATLSS Drive
Bethlehem, PA 18015-4729

Phone: (610)758-3525
Fax: (610)758-5902

www.atlss.lehigh.edu
Email: inatl@lehigh.edu

Table of Contents

EXECUTIVE SUMMARY

The SR 1045 Hares Hill Road Bridge was built in 1869 in Chester County, Pennsylvania by Moseley Iron Bridge and Roof Company. The bridge has been in service for approximately 136 years and has undergone a number of rehabilitation programs to its superstructure. The bridge's age, unique design, and historic significance, prompted engineers at PENNDOT to initiate an investigation to study the bridge's overall behavior and global response through controlled load testing and long-term monitoring.

Prior to testing, instrumentation plans were developed by researchers at the ATLSS Center with aid from engineers at Mackin Engineering Company. Key locations were chosen for installation of the instrumentation and included the Z-Bar arches, floorbeam flanges, diagonal and vertical strut of the queen post, lower and strengthening tie plates, lattice infilling, floorbeam connection plate, floorbeam connection rod, bottom flange of stringers, and diagonal tension bar. Two test trucks with known weights were used in the controlled load tests (single axle truck (lighter truck) and a tandem axle truck (heavier truck). The tests consisted of a series of five parked tests, eight crawl tests, and two dynamic tests. Both test trucks were fully loaded with gravel. The gross vehicle weight (GVW) of the lighter truck and the heavier truck was 35,300 pounds and 51,450 pounds, respectively. In addition to controlled load testing, uncontrolled monitoring was also conducted for a period of 3.2 days. The data were collected as random vehicles crossed the bridge.

Examining the data collected during the controlled load testing and the uncontrolled monitoring suggests that the bridge behaves as a tied arch bridge. None of the instrumented locations showed unexpectedly large response during monitoring.

In addition to the field study, an assessment of the material properties of the wrought-iron used in the bridge construction and the steel used in subsequent bridge rehabilitation was made by performing material testing on pieces extracted from the bridge. The material assessment is included in Appendix B and Appendix C of this report.

1.0 Project Summary and Background

1.1 Introduction

The Hares Hill Road Bridge is a single span wrought-iron tied arch with lattice infilling (truss members). It was built in 1869 in Chester County, Pennsylvania by Moseley Iron Bridge and Roof Company and it is the only known surviving example of its kind. The bridge crosses French Creek connecting Kimberton and Spring Cities. Figure 1.1 shows an elevation view of the bridge over French Creek.

Figure 1.1 – Elevation view of the Hares Hill Road Bridge over French Creek
(View looking west)

The bridge has been in service for approximately 136 years and has undergone a number of rehabilitation programs to its superstructure. The bridge's age, unique design, and historic significance, prompted engineers at PENNDOT to initiate an investigation to study the bridge's overall behavior and global response. As part of the study, researchers at the ATLSS Center of Lehigh University were contracted by the firm of Mackin Engineering Company at the direction of PENNDOT to conduct a field study of the bridge to assess its response to trucks with known weight through control load testing as well as to investigate its response to random live load traffic. In addition to the field study, an assessment of the material properties of the wrought-iron used in the bridge construction and the steel used in subsequent bridge rehabilitation was made by performing material testing on pieces of steel extracted from the bridge. Results of Material testing can be found in Appendix B and Appendix C.

To capture data needed to understand the bridge's overall behavior and response, strain gages were installed at various locations on the bridge. The location of the sensors was selected to capture the maximum response of the bridge superstructure to moving loads as well as the load distribution among the structural elements.

The field work was conducted from May 16 to May 18, 2005 by personnel from the ATLSS Center at Lehigh University, Bethlehem, PA.

2.0 Instrumentation Plan and Data Acquisition

The instrumentation plan used for both the controlled truck load testing and the random monitoring of live load traffic is described in the following section. The instrumentation plans were developed by ATLSS researchers, with aid from engineers at Mackin Engineering Company, to capture the maximum response of the structural elements of the bridge (eg. stringers, floorbeams, lattice infilling, queen post, etc.). A detailed description of the location of the strain gages installed on the bridge can be found in Appendix A.

2.1 Strain Gages

Strain gages were installed to understand the global response of the bridge as well as the local response at some details. Weldable gages type LWK-06-W250B-350, with an active grid length of 0.25 inches were used. The weldable gages were pre-bonded to a metal strip by the manufacturer and spot welded to the tested structure in the field.

Prior to installing the gages, the metal surfaces were ground and cleaned. After installation, the gages were covered with multi-layer system then sealed with a silicon type material.

The gages were produced by Measurements Group Inc. and are temperature-compensated for use on structural steel. The gage resistance is 350Ω and an excitation voltage of ten volts was used.

2.2 Data Acquisition

A Campbell Scientific CR9000 Data Logger was used for the collection of the data throughout the controlled testing. The logger is a high-speed, multi-channel, 16-bit system configured with digital and analog filters to help assure noise-free signals. Real-time data were viewed on site by connecting a laptop computer to the logger. Viewing real-time data while on site permitted ATLSS researchers to check that all sensors were functioning properly prior to conducting the controlled load testing and the uncontrolled monitoring.

2.3 Uncontrolled Monitoring

The CR9000 was also used for the uncontrolled monitoring of the bridge. The bridge was monitored for 3.2 days. During that phase, both time-history data and stress-range histograms were recorded.

To minimize the volume of data collected during recording of the stress-time-history files, a predefined lower limit stress value (i.e., trigger) for a particular gage was used to control when recording of the data began and ended. Once the stress value for that gage reached the predefined limit, the logger began recording data for all sensors installed on the bridge.

Based on the results of the controlled load tests and the monitoring of random traffic while on site, stress-range histograms were developed at selected locations. The stress-range histograms were divided into 0.5 ksi bins. Unlike the time history data, the stress-range histograms did not operate on triggers and were recorded continuously. Hence, all cycles were counted.

3.0 Controlled Load Testing

A series of controlled load tests were conducted using a single axle truck (lighter truck) and a tandem axle truck (heavier truck). Both test trucks were fully loaded with gravel. The gross vehicle weight (GVW) of the lighter truck and the heavier truck was 35,300 pounds and 51,450 pounds, respectively. Figure 3.1 shows the lighter truck, while Figure 3.2 shows the heavier truck. Also shown in the figures are the portable scales, which are under the tires, used to weigh the truck(s) axles on site. The geometry and the axle load data of the single axle truck are listed in Table 3.1 and Table 3.2, respectively. Similarly, the geometry and the axle load data of the tandem axle truck are listed in Table 3.3 and Table 3.4, respectively.

Figure 3.1 – The single axle truck (lighter truck) used in the controlled load testing

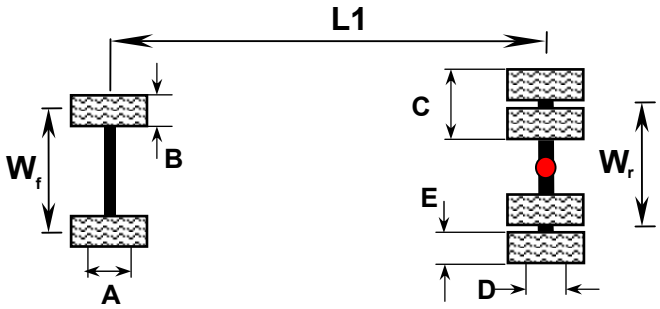

Rear Axle	L1 (in)	W_f (in)	W_r (in)	A[1] (in)	B (in)	C (in)	D[1] (in)	E (in)
Tandem	168	84	72	-	12	30	-	12

Note:
1. Parameter not measured

Table 3.1 – Geometry of the single axle truck (lighter truck) used in the controlled load tests

Test Description	Rear Axle Type	Front Axle Load (lb)	Rear Axle Load (lb)	GVW[1] (lb)	Date of Tests
Controlled Load Tests	Single	11,700	23,600	35,300	May 18, 2005

Note:
1. GVW = Gross Vehicle Weight

Table 3.2 – Axle load data of the single axle truck (lighter truck)

Figure 3-2 – The tandem axle truck (heavier truck) used in the controlled load testing

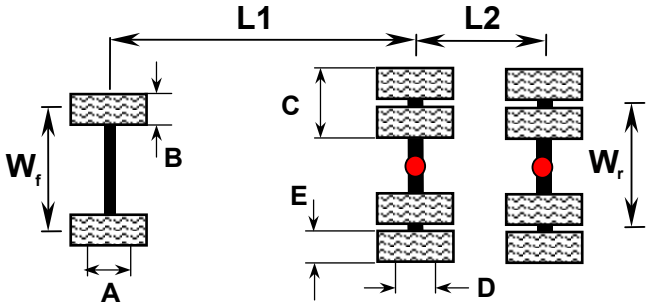

Rear Axle	L1 (in)	L2 (in)	W_f (in)	W_r (in)	A[1] (in)	B (in)	C (in)	D[1] (in)	E (in)
Tandem	162	51	85.50	74	-	14.50	22	-	8

Note:
1. Parameter not measured

Table 3.3 – Geometry of the tandem truck (heavier truck) used in the controlled load tests

Test Description	Rear Axle Type	Front Axle Load (lb)	Rear Axle Group Load (lb)	GVW[1] (lb)	Date of Tests
Controlled Load Tests	Tandem	14,450	37,000	51,450	May 18, 2005

Note:
1. GVW = Gross Vehicle Weight

Table 3.4 – Axle load data of the tandem truck (heavier truck)

The controlled load tests were conducted on May 18, 2005 between 9 AM and 12 PM. During the testing period, the bridge was closed to traffic by the Pennsylvania State Police to eliminate any disruption to the test program. The tests consisted of a series of five park tests, eight crawl tests, and two dynamic tests.

Two of the five park tests were conducted using the single axle truck. The remaining three tests were conducted using the tandem axle truck. In all park tests, the truck was driven onto the bridge and parked over floorbeam 7 and floorbeam 8. Recording of the data began when the rear axle was located directly above floorbeam 7. The truck was parked over floorbeam 7 for approximately 30 to 40 seconds, and then driven north and stopped over floorbeam 8 for about 30 to 40 seconds. In each park test the truck was positioned differently in the transverse direction to investigate the effect of the truck location on the local and global response of the Bridge. The top roadway of the bridge was marked by ATLSS personal using duct tape. The duct tape was used to guide the truck driver and to assure proper truck positioning while testing. A summary of the location of the test truck in the parked tests can be found in Table 3.5.

Seven of the eight crawl tests were conducted using the single axle test truck and one test was conducted using the tandem axle test truck. The single axle truck was moving forward from the south abutment towards the north abutment in six of the tests. In the seventh crawl test, the same test truck was moving backwards from the north abutment towards the south abutment. The last crawl test was conducted with the tandem axle truck moving backwards from the north abutment towards the south abutment. The truck was driven at a speed of approximately 3-5 miles per hour across the bridge in all crawl tests. In each test the truck was positioned differently in the transverse direction to capture the effect of changing the truck position on the response of the instrumented locations. Duct tape on the roadway was used to guide the truck driver to achieve the desired truck position while crossing the bridge. A summary of the exact location of the test truck can be found in Table 3.5.

Two dynamic tests were conducted using the single axle truck. The truck was traveling north at speed of approximately 15 miles per hour in the first test and south at a speed of approximately 17 mph in the second test. A summary of the exact location of the test truck can be found in Table 3.5.

3.1 Summary of Controlled Load Tests

The controlled load tests were performed on the Hares Hill Bridge on May 18, 2005. A summary of the controlled load tests is presented in Table 3.5.

Test	Speed (mph)	Direction	Truck Type	Comments
SACR_1.Dat	Very slow	North (moving forward)	Single Axle	Rear axle on instrumented stringers (CH_27 and CH_28)
SACR_2.Dat	Very slow	North (moving forward)	Single Axle	Rear axle on inside stringers (Slightly upstream)
SACR_3.Dat	~3-5 mph	South (backing up)	Single Axle	N/A
SACR_4.Dat	5	North (moving forward)	Single Axle	Roughly centered
SACR_5.Dat	5	North (moving forward)	Single Axle	Right dual centerline is located above CH_26
SACR_6.Dat	~3-5 mph	North (moving forward)	Single Axle	Right dual centerline is located above CH_27
SACR_7.Dat	5	North (moving forward)	Single Axle	Right dual centerline is located above CH_28
SAPK_1.Dat	N/A (Park Test)	N/A	Single Axle	Truck centered on the deck (59" from centerline of the truss to the centerline of the right dual) and parked on FLBM 7 and FLBM 8, respectively. Rear axle directly above the FLBM's.
SAPK_2.Dat	N/A (Park Test)	N/A	Single Axle	Truck hugging the right curb (27" from centerline of truss to the centerline of the right dual) and parked on FLBM 7 and FLBM 8, respectively. Rear axle directly above the FLBM's.
DYN_1.Dat	15	North (moving forward)	Single Axle	N/A
DYN_2.Dat	17	South (moving forward)	Single Axle	Front left tire was centered above CH_27
TAPK_1.Dat	N/A (Park Test)	N/A	Tandem Axle	Truck centered on the deck (59" from centerline of truss to the centerline of the right dual) and parked on FLBM 7 and FLBM 8, respectively. Rear axle directly above the FLBM's.
TAPK_2.Dat	N/A (Park Test)	N/A	Tandem Axle	Truck hugging the right curb (33" from centerline of truss to the centerline of the right dual) and parked on FLBM 7 and FLBM 8, respectively. Rear axle directly above the FLBM's.
TAPK_3.Dat	N/A (Park Test)	N/A	Tandem Axle	Truck hugging the left curb (37" from centerline of truss to the centerline of the right dual) and parked on FLBM 7 and FLBM 8, respectively. Rear axle directly above the FLBM's.
TACR_1.Dat	~3-5 mph	South (backing up)	Tandem Axle	N/A

Table 3.5 – Summary of the controlled load tests

4.0 Summary of Instrumentation Layout

The following section summarizes the instrumentation plan used on the bridge. Detailed instrumentation plans are included in Appendix A.

4.1 Strain Gages on Structural Elements

A total of 32 strain gages were installed on various structural wrought-iron and steel elements on the bridge. The locations selected for the gage installation were chosen such that the overall behavior and/or global response of the bridge could be examined. Such locations include the Z-Bar arches, the floorbeam flanges, the diagonal and vertical struts of the queen post attached to the bottom flange of floorbeam 8, lower and strengthening tie plates, lattice infilling, a floorbeam connection plate, floorbeam connection rods, bottom flanges of stringers, and a diagonal tension bar.

4.1.1 Strain Gages on the Z-Bar Arches

To investigate the response of the Z-Bar arches to moving loads, strain gages were installed on the top and bottom faces (back-to-back) of the Z-Bars. Gages were installed to capture any vertical or lateral out-of-plane bending that might exist in the arch. Specifically, CH_1 and CH_3 were installed on the top face of the west and east Z-Bars, respectively, (on the east arch of the bridge, east side of the bridge) and CH_2 and CH_4 were installed on the opposite face of the same Z-Bars, directly behind the installed gages (i.e. CH_2 was installed behind CH_1 and CH_4 was installed behind CH_3). Channels CH_24 and CH_25 were installed on the east Z-Bar (on the west arch of the bridge, west side of the bridge), where CH_24 was installed on the top face and CH_25 on the bottom face (directly behind CH_24) (only vertical bending could be measured on the west arch). All gages were installed on the Z-Bars at 1 inch from the edge of the bars and approximately 3 inches south of floorbeam 8. Figure 4.1 shows CH_24 installed on the top face of the west Z-Bar.

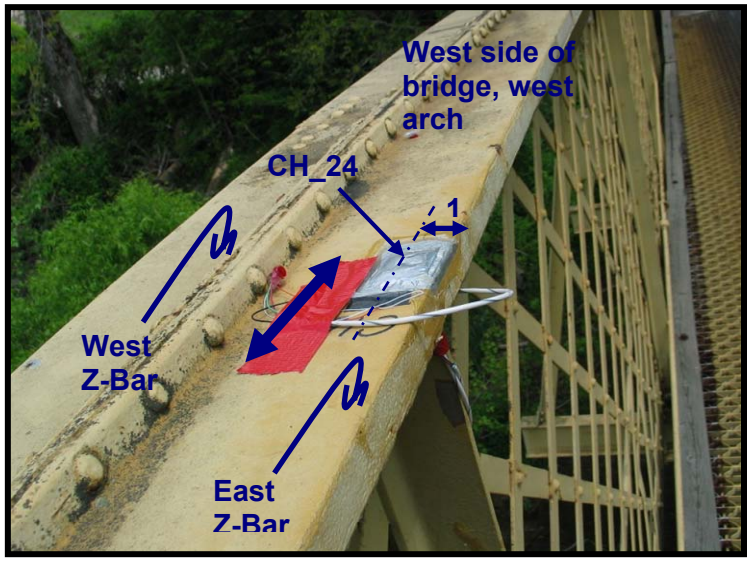

Figure 4.1 – CH_24 installed on the top face of the east Z-Bar on the west side of the bridge, approximately 1 inch from the edge of the bars and 3 inches south of floorbeam 8 (View looking north)

4.1.2 Strain Gages on Floorbeam Flanges

Strain gages were installed on the top and bottom flanges of floorbeam 7 and floorbeam 8 to capture the global response of the floorbeams. Channel CH_5 was installed on the top flange of floorbeam 8, while CH_6 was installed on the bottom flange of the same floorbeam. Similarly, CH_9 was installed on the top flange of floorbeam 7 and CH_10 was installed on the bottom flange of same floorbeam. Channels CH_5 and CH_9 were installed on the bottom face of the top flange at 1 inch from the flange edge and at mid span of the floorbeams. Channels CH_6 and CH_10 were installed on the centerline of the bottom face of the bottom flange at mid span of the floorbeams. Figure 4.2 shows CH_5 and CH_6 installed on the top and bottom flanges, respectively, of floorbeam 8.

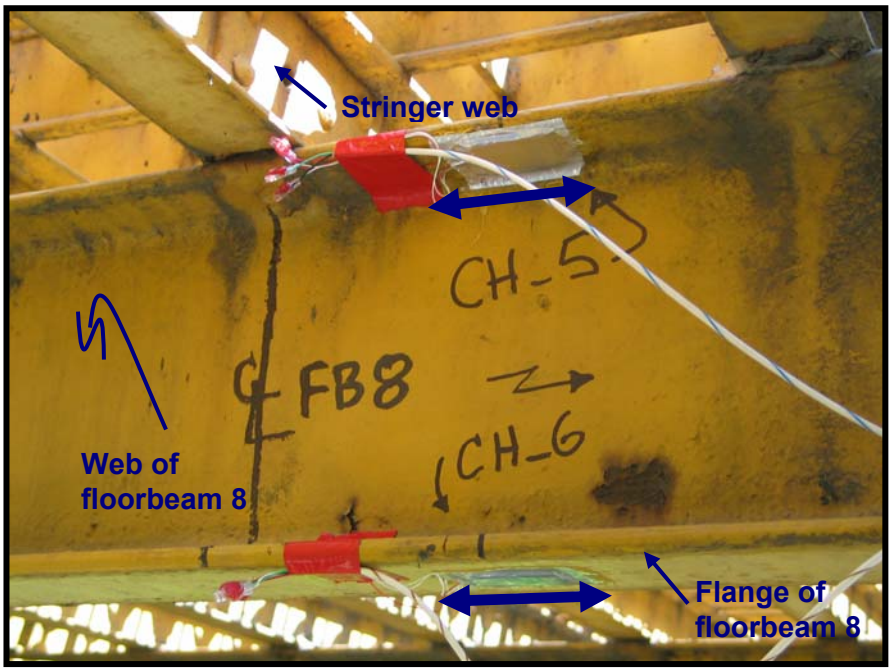

Figure 4.2 – CH_5 installed at mid span of floorbeam 8 on the bottom face of the top flange of the floorbeam and CH_6 installed at mid span of the same floorbeam on the bottom face of the bottom flange.
(View looking south)

It is important to mention that floorbeam 8 is typical of the existing floorbeams, which are made of wrought-iron and are part of the as-built condition of the bridge. Floorbeam 7, however, represents floorbeams made of conventional structural steel, which were added to the bridge as part of a previous rehabilitation program. Every added floorbeam was installed between two existing floorbeams. For example floorbeam 7 was installed between the existing floorbeam 6 and floorbeam 8. These two types of floorbeams differ in their size and the type of attachment used to connect the floorbeam to the lower tie plate.

4.1.3 Strain Gages on Diagonal and Vertical Strut of the Queen Post

Diagonal and vertical struts of the queen posts are attached to the bottom flanges of the added floorbeams to strengthen the beams for vertical loads. Channels were installed on the vertical and diagonal struts of the queen post attached to the bottom flange of floorbeam 8 to investigate the mechanism by which load is being transferred through the diagonal and the queen post members. Channel CH_23 was installed on the front face (looking north) of the vertical strut at mid height (Figure 4.3), while CH_8 was installed on the top face of the diagonal strut at mid length (Figure 4.4). Channel CH_7 was installed directly behind CH_8 to capture the out-of-plane bending behavior in the diagonal member, if any.

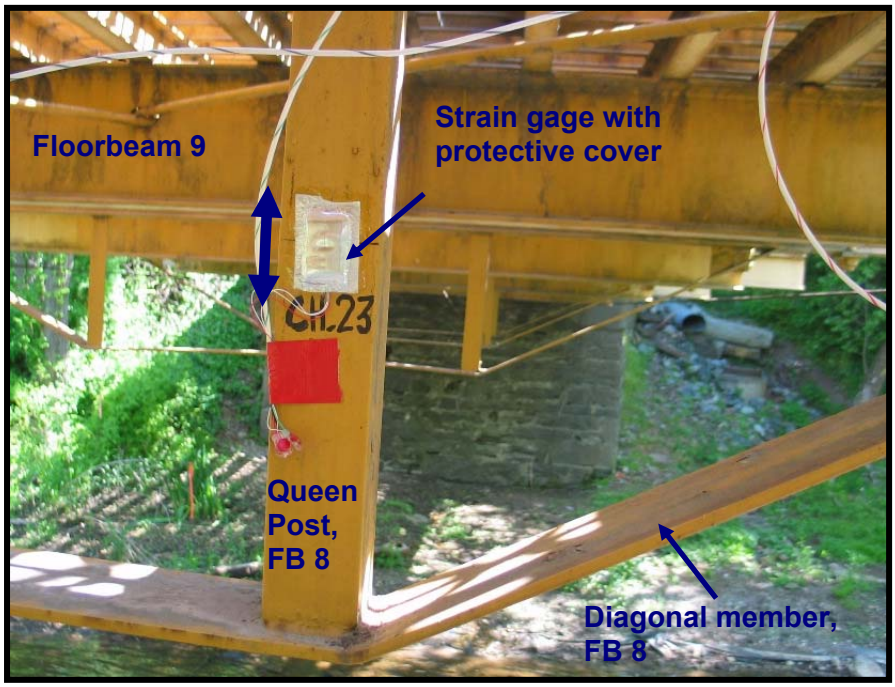

Figure 4.3 – CH_23 installed on the front face at mid height of the vertical strut attached to the bottom flange of floorbeam 8
(View looking north)

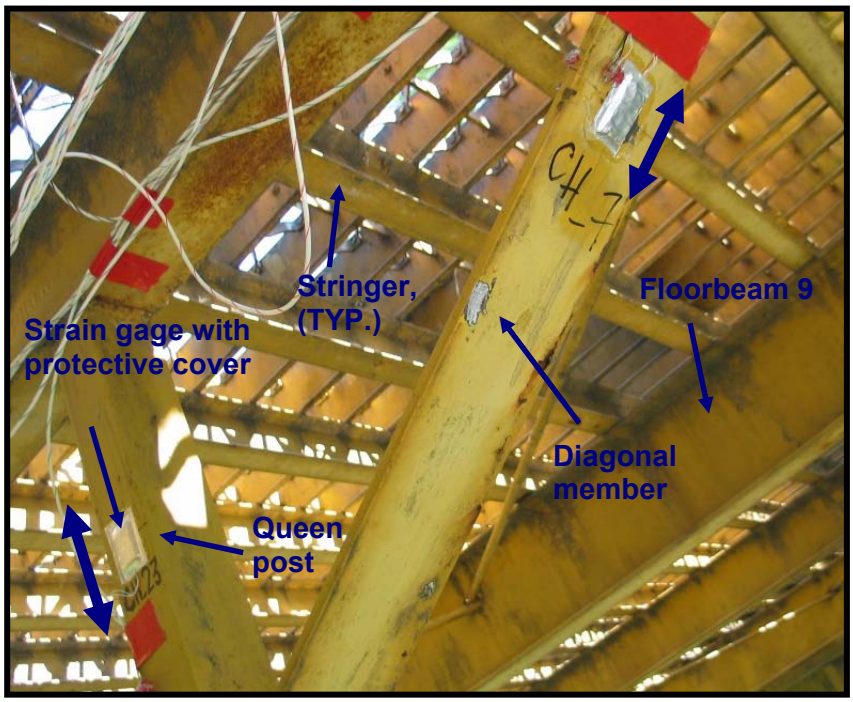

Figure 4.4 – CH_7 installed at mid length on the bottom face of the diagonal strut member. Channel CH_8 is installed on the opposite face of the diagonal member directly behind CH_7, not shown in the picture
(View looking north)

4.1.4 Strain Gages on Lower and Strengthening Tie Plates

The lower tie plate is used to tie both ends of the Z-Bar arch member together to restrain the horizontal forces at the end of the arch. Gages were installed on the top and bottom edges of the tie plate to measure the stresses in the plate. Specifically, CH_11 and CH_12 were installed on the top and bottom edge, respectively, of the lower tie plate on the east side of the bridge.

As previously mentioned the bridge's superstructure has undergone a number of rehabilitation programs. During on of these, strengthening plates were added adjacent to the existing tie plates. The plates were added to reduce the load carried by the existing tie plates. Channels CH_21 and CH_22 were installed on the top and bottom edges of the plate, respectively, between floorbeam 7 and floorbeam 8 to measure the stresses in the plate and investigate the degree by which the load is being shared between the existing tie plate and the strengthening plate. In addition, CH_29 and CH_30 were installed on the top and bottom edges, respectively, of the strengthening tie plate at 5'-4 1/2" away from the south end of the plate.

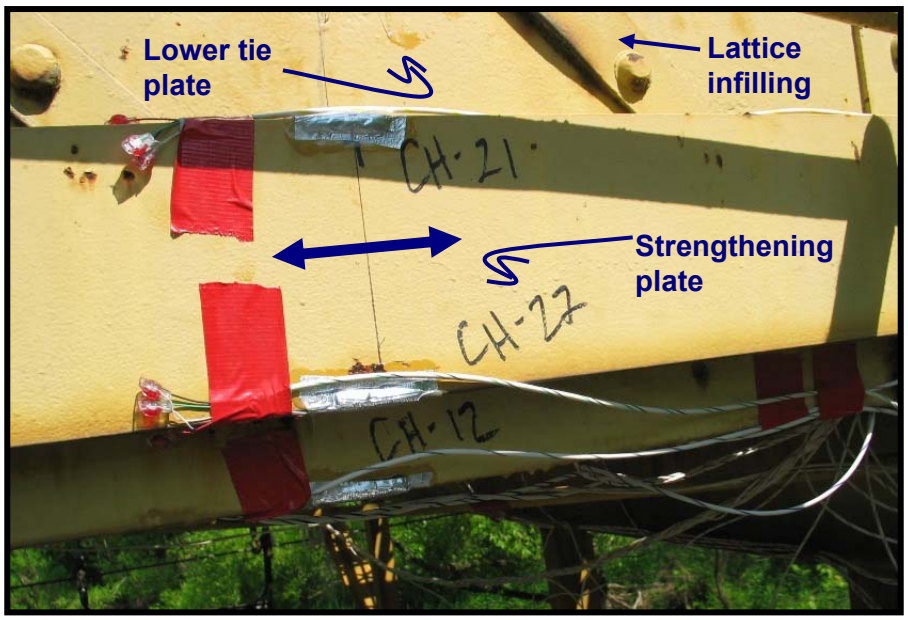

Figure 4.5 – CH_21 and CH_22 installed on the top and bottom edges, respectively, of the strengthening plate and CH_12 installed on the bottom edge of the existing tie plate (View looking west)

4.1.5 Strain Gages on Lattice Infilling

The lattice infilling acts primarily as a web and as truss members and assist in transferring the load from the lower tie plates to the arch members. Strain gages were installed on a randomly chosen lattice member to measure the stresses in the member. Channels CH_13 and CH_14 were installed back-to-back on a lattice approximately 14 inches from the intersection between the lattice and the vertical T-shape floorbeam hanger at mid span. The channels were installed back-to-back to measure any out-of-plane stresses in the member. Figure 4.6 shows CH_14 installed on the front face (looking west) of the lattice member. Channel CH_13 is installed on the back face of the member directly behind CH_14.

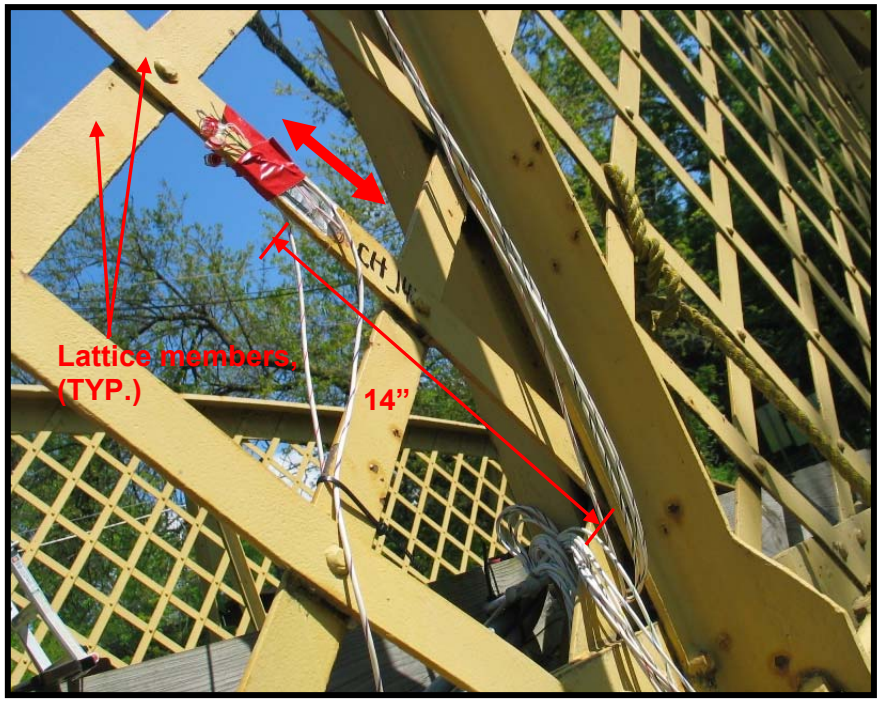

Figure 4.6 – CH_14 installed on the front face of the lattice member approximately 14 inches from the intersection between the lattice and the vertical T-shape member located at mid span (CH_13 is installed directly behind CH_14, not shown in the picture) (View looking west)

4.1.6 Strain Gages on Floorbeam Connection Plate

Bending stresses in the connection plate used for connecting the lower tie plate to floorbeam 7 were measured by installing a strain gage on both faces of the connection pate. The gages were installed on both sides to measure the out-of-plane stresses in the plate. The gage on the back face (CH_16) was installed between the top end of the angle connecting the floorbeam web to the connection plate and the horizontal line of bolts connecting the lower tie plate to the connection plate. After installing CH_16, CH_15 was installed on the opposite face (front face) directly behind CH_16. Figure 4.7 and Figure 4.8 show CH_16 and CH_15, respectively.

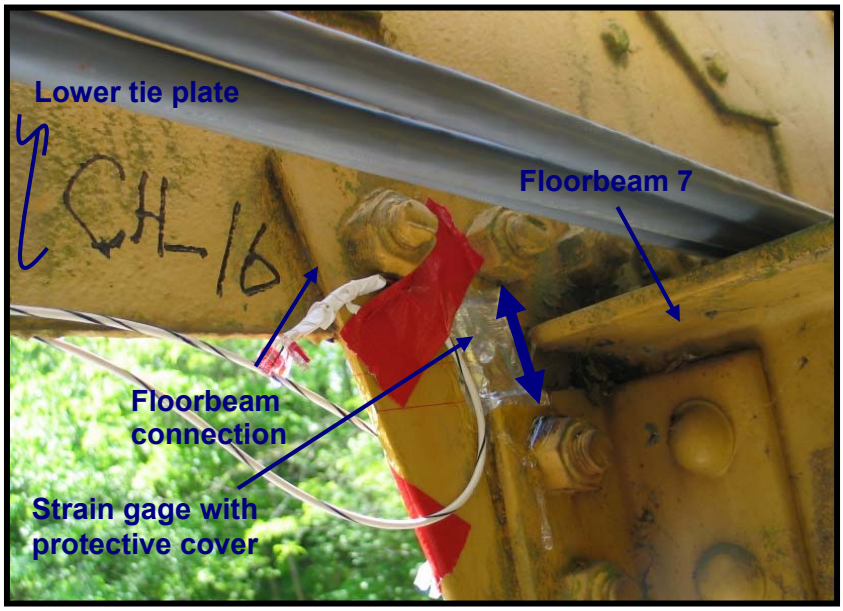

Figure 4.7 – CH_16 installed on the back face of the connection plate at floorbeam 7 (CH_15 installed directly behind CH_16, is not shown in the picture) (View looking east).

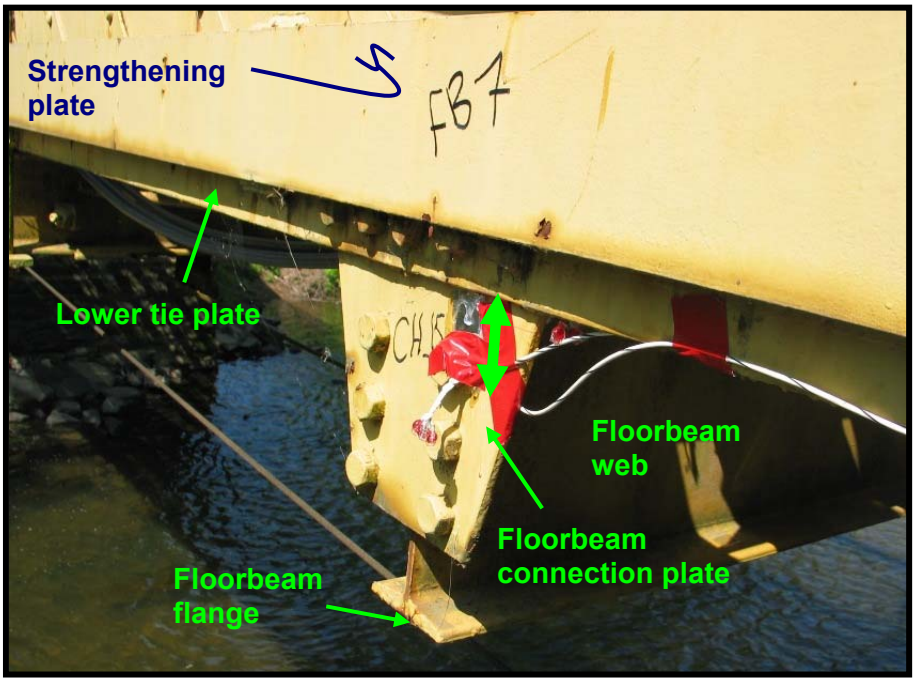

Figure 4.8 – CH_15 installed on the front face of the connection plate at floorbeam 7
(CH_16 installed directly behind CH_15, is not shown in the picture)
(View looking west)

4.1.7 Strain Gages on Floorbeam Connection Rods

Connection rods attach the lower tie plate to the existing floorbeams. Strain gages were installed on the rod to measure the stresses in the rod. The gages were installed back-to-back to measure the out-of-plane stresses in the rod as a result of the global deflection of the floorbeam. Channel CH_17 was installed on the exterior face (looking west) of the connection rod south of the web of floorbeam 8 (Figure 4.9). Channel CH_18 was installed on the interior face directly behind CH_17. Similarly, Channel CH_19 was installed on the exterior face (looking west) of the connection rod north of the web of floorbeam 8 and CH_20 was installed on the interior face directly behind CH_19.

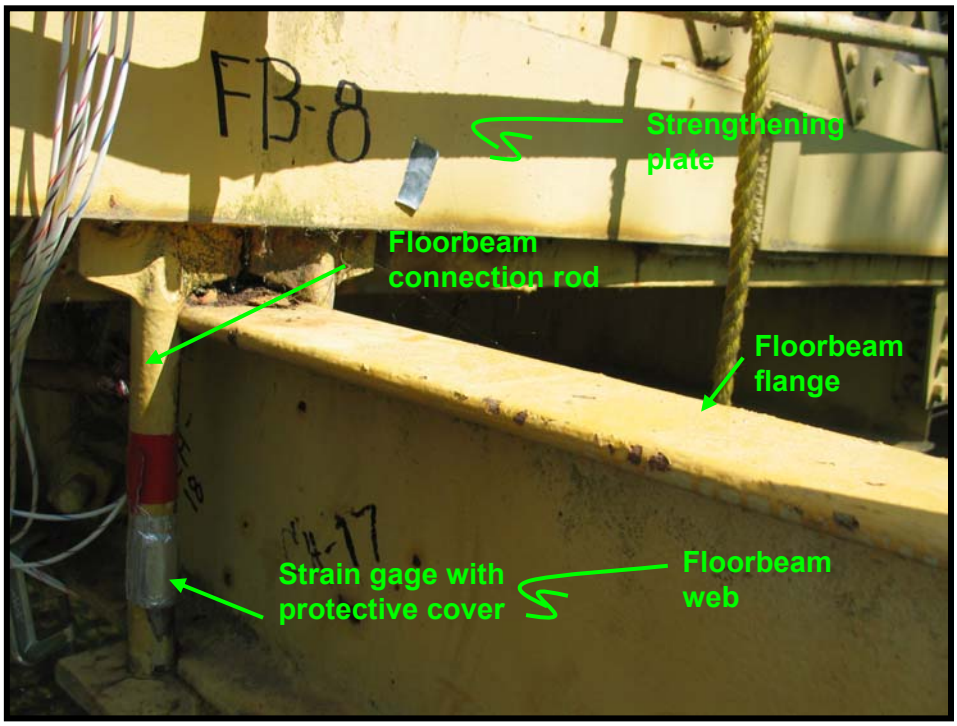

Figure 4.9 – CH_17 installed on the front face of the connection rod south of the web of floorbeam 8 (CH_18 installed directly behind CH_17, not shown in the picture) (View looking west)

4.1.8 Strain Gages on Bottom Flanges of Stringers

Strain gages were installed on the bottom flanges of three stringers to measure their response to moving load. The gages were installed on the bottom flanges of stringers S11, S10, and S9 (at the centerline of the flange) at the mid distance between floorbeam 7 and floorbeam 8. Specifically, CH_26 was installed on the bottom flange of stringer S11, CH_27 was installed on the bottom flange of stringer S10, and CH_28 was installed on the bottom flange of stringer S9. The gages were installed at adjacent stringers to study the effect of changing the transverse position of the test trucks on the global response in the stringers. In addition, the effect of a wheel load on the localized response in a given stringer flange could be investigated by comparing the response in all three flanges under a specific load. Finally, load distribution among the all three stringers could be studied by comparing their response to a given load. Figure 4.10 shows the three gages installed on the bottom face of the bottom flanges.

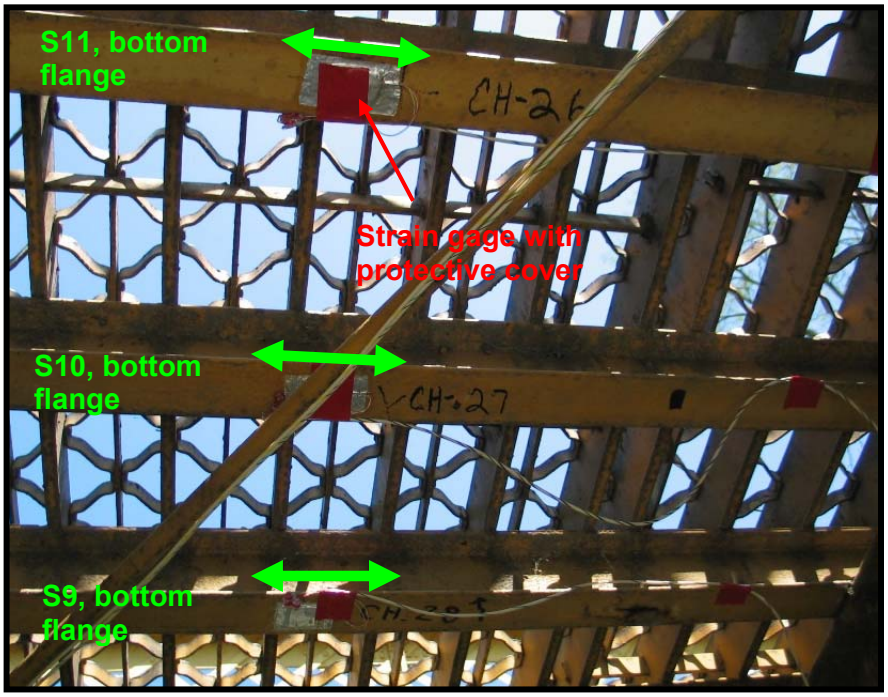

Figure 4.10 – CH_26, CH_27, and CH_28 installed on the bottom faces of the bottom flanges of stringers S11, S10, and S9, respectively.
(Underside view)

4.1.9 Strain Gages on Diagonal Tension Bar

Two strain gages were installed on the east diagonal tension bar, which ties the east Z-Bar arch near floorbeam 2 to the bottom end of the vertical T-shape member at floorbeam 8. Channel CH_31 was installed on the east face of the bar, while CH_32 was installed on the west face. The gages were installed at a diagonal distance of approximately 11'-6" away from the end of the bar at floorbeam 8. As shown in Figure 4.11, two gages were installed back-to-back on the rod to measure both the in-plane axial stresses and any the out-of-plane bending stresses that might exist.

Figure 4.11 – CH_31 and CH_32 installed on the east and west faces, respectively, of the diagonal tension bar, which ties the east Z-Bar arch near floorbeam 2 to the bottom end of the vertical T-shape member at floorbeam 8. The gages were installed at a diagonal distance of approximately 11'-6" away from the end of the bar at floorbeam 8.

5.0 Results of Controlled Load Tests

The results of the controlled static and dynamic load tests are discussed in this section.

5.1 General Response

In general, the bridge responded as a beam such that the arch and the tie plates could be considered as the top and bottom flange of a beam, respectively, and the lattice infilling could be considered as the web of the beam. The analogy is made based on the out-of-plane bending behavior of the lattice infilling (Section 5.7) and the in-plane bending behavior, along with axial tension, of the lower and strengthening tie plates. The bridge also responded as a tied arch. Compressive stresses were measured in the steel arch members as the test truck(s) crossed over the bridge. Figure 5.1 presents the response of CH_1 and CH_2 installed on the top and bottom face, respectively, of the west Z-Bar on the east side of the bridge, and CH_3 and CH_4 installed on the top and bottom face, respectively, of the east Z-Bar on the east side of the bridge, as the single axle test truck passed over the bridge in the crawl test (SACR_1). All four channels were installed 1 inch from the south end of the bar and approximately 3 inches south of floorbeam 8.

As seen in the figure, the response in CH_1 and CH_2 is almost identical, indicating that the stresses are in-plane (i.e. no vertical out-of-plane bending in the west Z-Bar member located on the east side of the bridge). It is important to mention that in all controlled tests, equal stresses were observed for CH_1 and CH_2 installed on the top and bottom face of the west Z-Bar located on the east side of the bridge. Similarly, equal stresses were observed for CH_24 and CH_25 installed on the top and bottom face on the east Z-Bar located on the west side of the bridge. Larger stresses were, however, measured in CH_3 and CH_4 installed on the top and bottom face of the east Z-Bar located on the east side of the bridge. In fact, the response of CH_3 and CH_4 was always higher than that of CH_1, CH_2, CH_24, and CH_25 in any of the controlled load tests suggesting lateral bending of the east arch under live load. Although the west arch on the west side of the bridge was not instrumented, lateral bending of the west arch may also be expected as a result of symmetry.

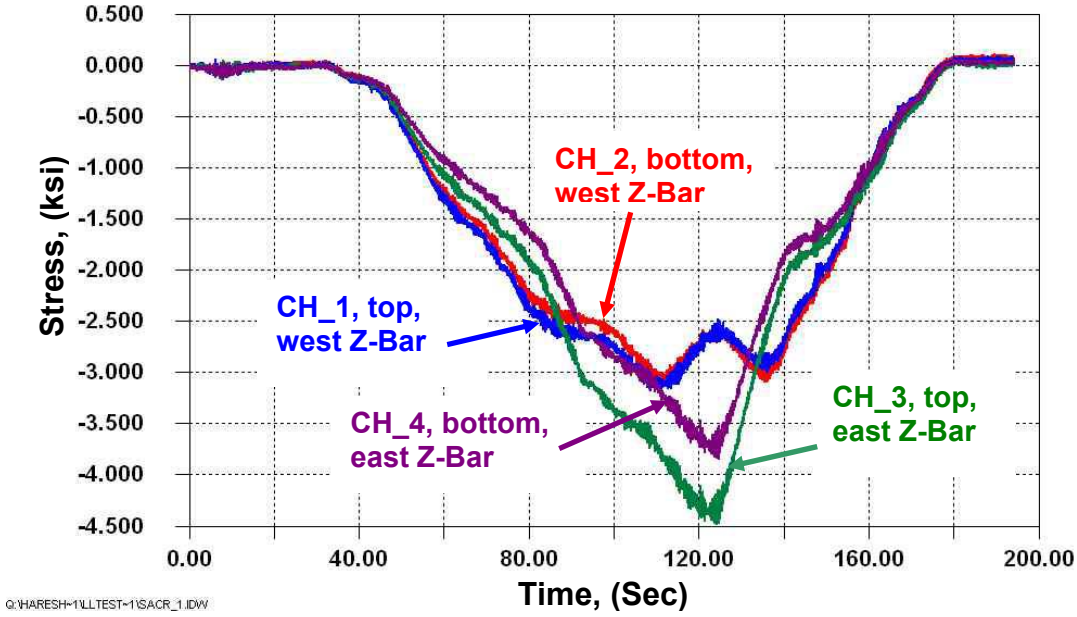

Figure 5.1 – Response of CH_1 and CH_2 installed on the top and bottom face, respectively, of the west Z-Bar on the east side of the bridge, and CH_3 and CH_4 installed on the top and bottom face, respectively, of the east Z-Bar on the east side of the bridge, as the single axle test truck passed over the bridge in the crawl test (SACR_1) (All four channels were installed inch from the edge of the bar and approximately 3 inches south of floorbeam 8)

Figure 5.2 shows the response of CH_11 and CH_12 installed on the top and bottom edge, respectively, of the lower tie plate on the east side of the bridge, as the single axle test truck passed over the bridge in the crawl test (SACR_1). As shown in the figure and as expected, tensile stresses are present in both the top and bottom edges of the tie plate. The difference in the magnitude of the measured stresses in both channels is believed to be due to bending stresses in the tie plates (tensile bending stresses in the bottom edge and compressive bending stresses in the top edge), which are superimposed onto the axial tensile stresses resulting in the total final stresses shown in Figure 5.2. The bending stresses in the tie plates is most likely the result of a global bending in the plate due to crossing of the truck(s). The localized response shown in the figure is believed to be the point at which only axial stresses are present in the lower tie plate at the instrumented location (i.e. no bending stress component).

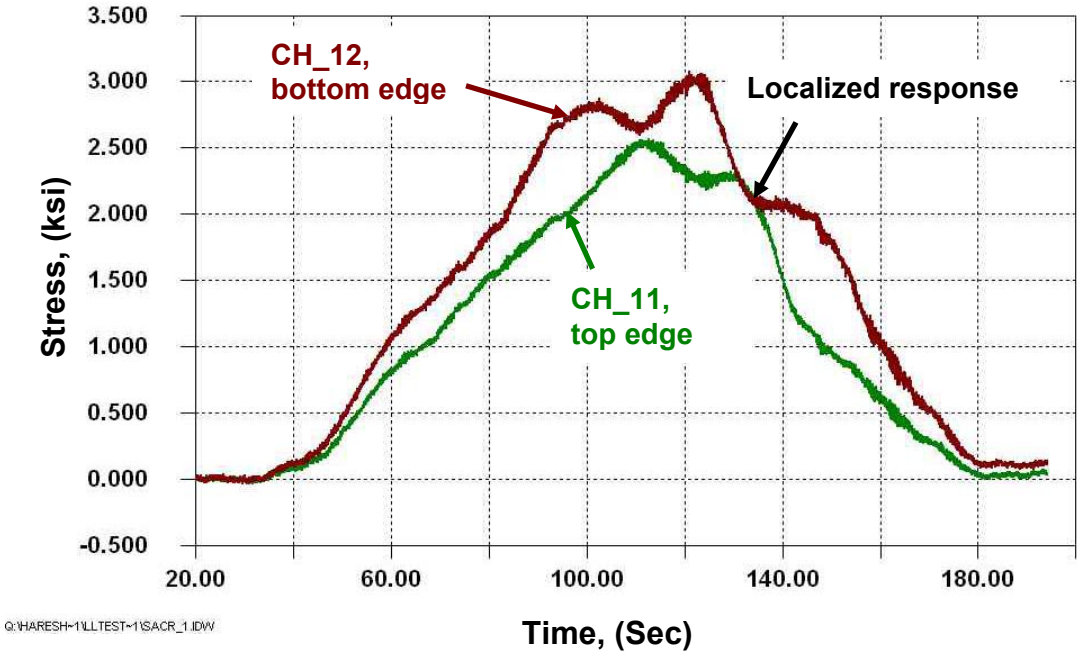

Figure 5.2 – Response of CH_11 and CH_12 installed on the top and bottom edges, respectively, of the lower tie plate on the east side of the bridge, as the single axle test truck passed over the bridge in the crawl test (SACR_1).

5.2 Repeatability of Data

All static, dynamic, and park tests were repeated. However, some parameters were altered within each repeated test to study the effect of changing the parameters on the behavior of the instrumented locations. The parameters altered were truck speed, direction, type, and position. Although changing these parameters had an effect on the magnitude of the measured stresses, the overall response in a given channel was consistent throughout all tests as discussed below.

5.3 Stresses in the Z-Bar Arches

Gages were installed on the top and bottom face, respectively, of the Z-Bars to measure the response of the arches to moving loads. Specifically, CH_1, CH_2, CH_3, and CH_4 were installed on the top and bottom faces of the Z-Bars located at the east side of the bridge, where CH_1 and CH_3 were installed on the top face of the west Z-Bar and east Z-Bar, respectively, on the east side of the bridge (east arch) and CH_2 and CH_4 were installed directly behind CH_1 and CH_3, respectively. On the west side of the bridge (west arch), CH_24 was installed on the top face of the east Z-Bar and CH_25 was installed on the bottom face of the same Z-Bar, directly behind CH_24.

Compressive stresses were measured in all strain gages installed on the face of the Z-Bars. As seen in Figure 5.3, similar response was observed in CH_1 installed on the top face of the west Z-Bar located on the east side of the bridge and CH_24 installed on the top face of the east Z-Bar located on the west side of the bridge. It is important to note that although the shape of the curve representing the response in CH_1 and CH_24 is the same in all repeated tests, the magnitude of the measured stresses varies depending on the transverse location of the test truck on the bridge in a given test. The figure also shows that, as mentioned earlier, the response in CH_3 is higher than that of CH_1 and CH_24. A summary of the maximum and minimum stress values from the strain gages installed on the top and bottom face of the Z-Bar arches in the crawl tests is presented in Table 5.1.

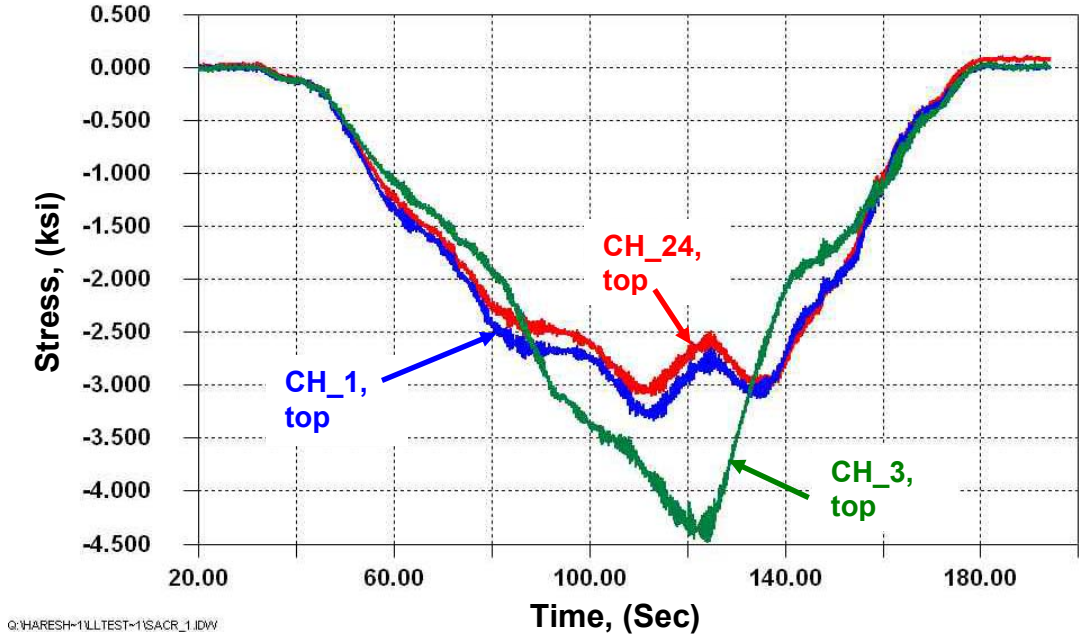

Figure 5.3 – Response of CH_1 and CH_24 installed on the top face of the east Z-Bars located on the east and west side of the bridge (east arch and west arch), respectively, and CH_3 installed on the top face of the west Z-Bar located on the east side of the bridge (east arch), as the single axle test truck passed over the bridge in the crawl test (SACR_1).

As previously mentioned in Section 5.1, the response of CH_3 and CH_4 was always higher than that of CH_1 and CH_2, suggesting that lateral bending stresses are present in the east arch and therefore, could also be assumed to be present in the west arch due to symmetry. To understand the response of the east arch, rather than the response of individual Z-Bars, to moving load, the response of channels CH_1 through CH_4 shown in Figure 5.1 was resolved into axial stress component, vertical bending stress component, and lateral bending stress component acting on the east arch as shown in Figure 5.4. As shown in the figure, the response of the east arch to moving load is primarily axial compressive stresses. The arch experiences lateral bending as previously suggested. It is however unclear as to why the lateral bending stress changes its sign as the test truck crossed over the bridge. The figure also shows that the east arch experiences small magnitude of compressive vertical bending stresses.

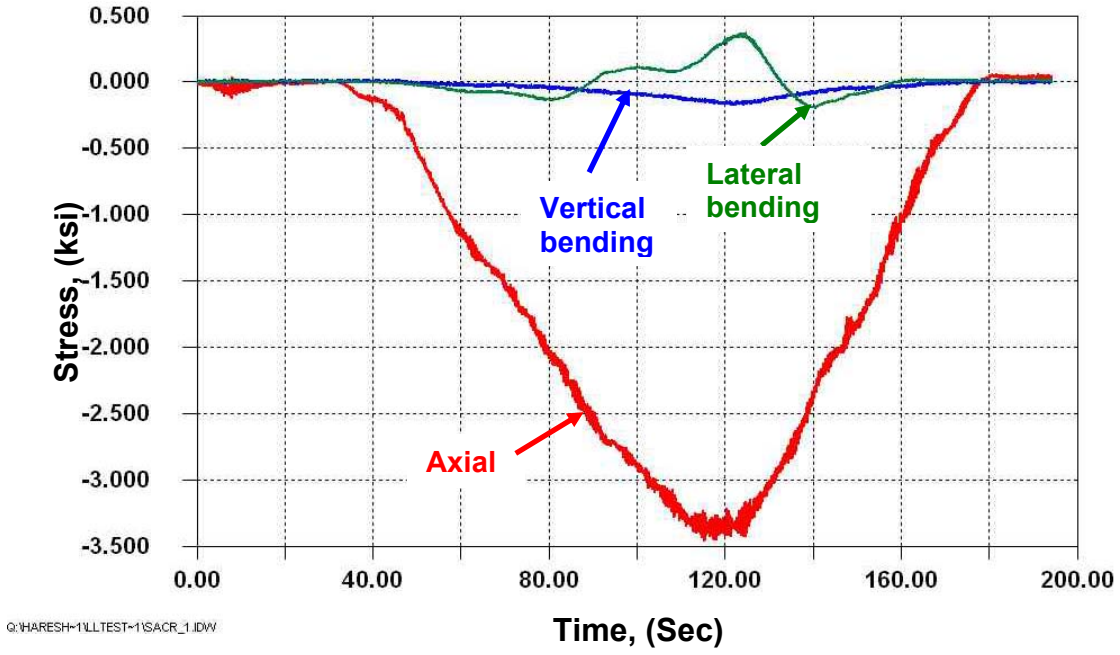

Figure 5.4 – Axial, vertical, and lateral stresses in the east arch as the single axle test truck passed over the bridge in the crawl test (SACR_1).

Test Designation	CH_1, East Z-Bar, top face of bar (ksi)		CH_2, East Z-Bar, bottom face of bar (ksi)	
	σ_{max}	σ_{min}	σ_{max}	σ_{min}
SACR_1.Dat	0.1	-3.1	0.1	-3.2
SACR_2.Dat	0.1	-3.0	0.1	-3.0
SACR_3.Dat	0.0	-3.2	0.0	-3.3
SACR_4.Dat	0.0	-3.5	0.0	-3.5
SACR_5.Dat	0.0	-4.1	0.0	-4.2
SACR_6.Dat	0.1	-3.4	0.0	-3.5
SACR_7.Dat	0.0	-2.9	0.0	-3.0
TACR_1.Dat	0.0	-5.0	0.0	-5.1

Test Designation	CH_3, West Z-Bar, top face of bar (ksi)		CH_4, West Z-Bar, bottom face of bar (ksi)	
	σ_{max}	σ_{min}	σ_{max}	σ_{min}
SACR_1.Dat	0.0	-4.4	0.0	-3.8
SACR_2.Dat	0.0	-4.2	0.0	-3.6
SACR_3.Dat	0.0	-4.5	0.0	-3.8
SACR_4.Dat	0.0	-4.7	0.0	-4.0
SACR_5.Dat	0.0	-5.4	0.0	-4.6
SACR_6.Dat	0.0	-4.6	0.0	-4.0
SACR_7.Dat	0.0	-4.2	0.0	-3.6
TACR_1.Dat	0.0	-6.6	0.0	-5.7

Test Designation	CH_24, East Z-Bar, top face of bar (ksi)		CH_25, East Z-Bar, bottom face of bar (ksi)	
	σ_{max}	σ_{min}	σ_{max}	σ_{min}
SACR_1.Dat	0.0	-3.3	0.1	-3.4
SACR_2.Dat	0.1	-3.5	0.1	-3.7
SACR_3.Dat	0.0	-3.2	0.0	-3.3
SACR_4.Dat	0.0	-3.0	0.0	-3.2
SACR_5.Dat	0.0	-2.4	0.0	-2.5
SACR_6.Dat	0.0	-3.0	0.0	-3.2
SACR_7.Dat	0.0	-3.5	0.0	-3.6
TACR_1.Dat	0.0	-4.3	0.0	-4.4

Table 5.1– Summary of peak measured stresses in CH_1, CH_2, CH_3, and CH_4 installed on the east and west Z-Bar (on the east side of the bridge) and CH_24 and CH_25 installed on the east Z-Bar (on the west side of the bridge) for the various test truck transverse positions in the crawl tests.

5.4 Stresses in Floorbeam Flanges

A typical response of the strain gages installed on the top and bottom flanges of floorbeam 7 and floorbeam 8 during the controlled load testing is shown in Figure 5.5. Channels CH_5 and CH_6 were installed on the bottom and top flange, respectively, of floorbeam 8 and CH_9 and CH_10 were installed on the bottom and top flange, respectively, of floorbeam 7. All four channels were installed at mid span of the floorbeams. As shown in the figure, tensile stresses were measured in the bottom flanges and compressive stresses were measured in the top flanges. The response of the strain gages installed on floorbeam 7 (added to the bridge) is higher than that installed on floorbeam 8 (existing floorbeam). A summary of the maximum and minimum stress values from the strain gages installed on the top and bottom flange of floorbeam 7 and floorbeam 8 in the crawl tests is presented in Table 5.2. It is clear from the table that altering the transverse position of the single axle test truck in the controlled crawl tests had very minimal effect on the magnitude of the measured stresses at a given strain gage (i.e. the response in CH_1 is almost identical in all crawl tests regardless of the transverse position on the test truck). The table also shows that the stresses in the bottom and top flanges of floorbeam 8 are lower than that of floorbeam 7, suggesting that the vertical and diagonal queen posts of floorbeam 8 help in strengthening the floorbeam and participate in carrying of the vertical load imposed on the floorbeam.

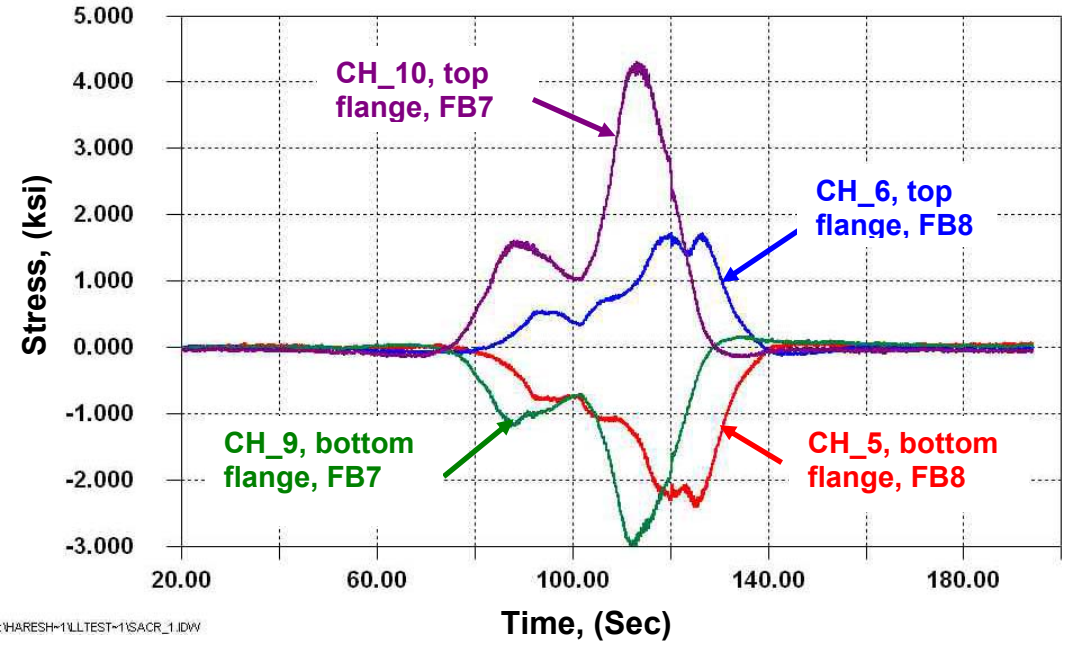

Figure 5.5 – Response of CH_5 and CH_6 installed on the bottom and top flange of floorbeam 8, respectively, and CH_9 and CH_10 installed on the bottom and top flange, respectively, of floorbeam 7 as the single axle test truck passed over the bridge in the crawl test (SACR_1).

Test Designation	CH_5, FB8, bottom flange (ksi)		CH_6, FB8, top flange (ksi)	
	σ_{max}	σ_{min}	σ_{max}	σ_{min}
SACR_1.Dat	0.1	-2.4	1.7	-0.1
SACR_2.Dat	0.0	-2.4	1.7	-0.1
SACR_3.Dat	0.1	-2.3	1.7	-0.1
SACR_4.Dat	0.1	-2.3	1.6	-0.1
SACR_5.Dat	0.0	-2.4	1.8	-0.1
SACR_6.Dat	0.0	-2.3	1.6	-0.1
SACR_7.Dat	0.0	-2.4	1.7	-0.1
TACR_1.Dat	0.0	-3.5	2.4	-0.1

Test Designation	CH_9, FB7, bottom flange (ksi)		CH_10, FB7, top flange (ksi)	
	σ_{max}	σ_{min}	σ_{max}	σ_{min}
SACR_1.Dat	0.2	-3.0	4.2	-0.2
SACR_2.Dat	0.2	-3.0	4.4	-0.1
SACR_3.Dat	0.1	-3.0	4.0	-0.2
SACR_4.Dat	0.2	-3.0	4.2	-0.1
SACR_5.Dat	0.1	-2.9	4.2	-0.1
SACR_6.Dat	0.1	-2.9	4.3	-0.1
SACR_7.Dat	0.1	-3.0	4.3	-0.1
TACR_1.Dat	0.2	-4.1	5.9	-0.2

Table 5.2– Summary of peak measured stresses in the CH_5, CH_6, installed on the bottom and top flange, respectively, of floorbeam 8 and CH9, and CH_10 installed on the bottom and top flange, respectively, of floorbeam 7 for the various test truck transverse positions in the crawl tests.

5.5 Stresses in Diagonal and Vertical Strut of the Queen Post

Channels CH_7 and CH_8 were installed on the bottom face and top face, respectively, of the diagonal strut attached to the bottom flange of floorbeam 8. The strain gages were installed back-to-back to measure any out-of-plane bending in the diagonal member. Tensile stresses of approximately equal magnitude were measured in both channels in the controlled load tests indicating that a very small out-of-plane bending was present in the diagonal strut. Figure 5.6 shows a typical response of CH_7 and CH_8 during the controlled load test (SACR_1).

The response of the vertical strut to moving load is also shown in Figure 5.6. Channel CH_23 was installed on the front face of the vertical strut attached to the bottom flange of floorbeam 8. Compressive stresses were measured in the vertical member during all tests. Table 5.3 lists a summary of the maximum and minimum stress values experienced by the channels installed on the diagonal and vertical strut of the queen post during the crawl tests. As the table indicates, the response in both the diagonal and vertical strut of the queen post was consistent in all crawl tests, indicating that changing the truck position in the crawl tests had a minimal effect on the response in the instrumented struts.

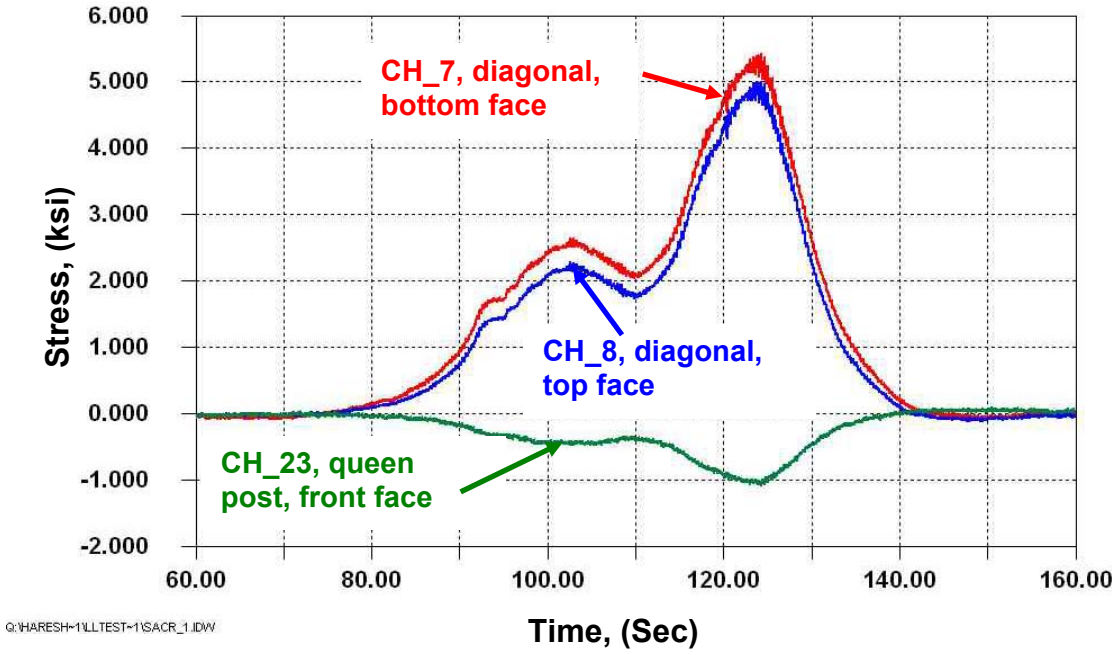

Figure 5.6 – Response of CH_7 and CH_8 installed on the bottom and top face of the diagonal member attached to floorbeam 8 and the response of CH_23 installed on the front face of the queen post member attached to floorbeam 8 as the single axle test truck passed over the bridge in the crawl test (SACR_1).

Test Designation	CH_7, diagonal strut, top face (ksi)		CH_8, diagonal strut, bottom face (ksi)	
	σ_{max}	σ_{min}	σ_{max}	σ_{min}
SACR_1.Dat	5.4	-0.1	4.9	-0.1
SACR_2.Dat	5.2	0.0	4.9	0.0
SACR_3.Dat	5.3	-0.1	4.9	0.0
SACR_4.Dat	5.3	0.0	5.0	0.0
SACR_5.Dat	5.0	-0.1	4.5	-0.1
SACR_6.Dat	5.4	-0.1	4.9	-0.1
SACR_7.Dat	5.2	-0.1	4.8	-0.1
TACR_1.Dat	7.0	-0.0	6.5	-0.0

Test Designation	CH_23, vertical strut, front face (ksi)	
	σ_{max}	σ_{min}
SACR_1.Dat	0.1	-1.1
SACR_2.Dat	0.1	-1.1
SACR_3.Dat	0.1	-1.0
SACR_4.Dat	0.1	-1.0
SACR_5.Dat	0.0	-0.9
SACR_6.Dat	0.1	-1.0
SACR_7.Dat	0.0	-1.1
TACR_1.Dat	0.1	-1.4

Table 5.3– Summary of peak measured stresses in CH_7 and CH_8 installed on the bottom and top face, respectively, of the diagonal strut of the queen post attached to floorbeam 8 and CH_23 installed on the front face of the vertical strut of the queen post attached to the same floorbeam for the various test truck transverse positions in the crawl tests

5.6 Stresses in the Lower and Strengthening Tie Plates

Four gages were installed on the top and bottom edges of the original lower tie plate and strengthening plate at mid distance between floorbeam 7 and floorbeam 8 to investigate their response to moving load. Channels CH_11 and CH_12 were installed on the top and bottom edges, respectively, of the original tie plate at mid distance between floorbeam 7 and floorbeam 8. Similarly, CH_21 and CH_22 were installed on the top and bottom edges, respectively, of the strengthening plate at mid distance between floorbeam 7 and floorbeam 8. In addition, two gages, CH_29 and CH_30, were installed on the top and bottom edges of the strengthening plate approximately 5'-4 1/2" away from the south end of the plate.

Tensile stresses were measured in the top and bottom edges of the instrumented lower tie plate and strengthening plate, on the east side of the bridge. As shown in Figure 5.7 and in Table 5.4, equal stress values were measured in CH_12 and CH_22 installed on the bottom edges of the tie plate and the strengthening plate, respectively. The response of CH_11 installed on the top edge of the tie plate was approximately 13%, on average, higher than that of CH_21 installed on the top edge of the strengthening plate. It is practical to say that equal response was also observed in CH_11 and CH_21 installed on the top edge of the plates. However, it is important to point out that the measured stresses in the plates are due to the axial stress component resulting from the tie plates restraining the horizontal forces at the end of the arch and the bending component resulting from global bending of the plates as the truck (s) crossed over the bridge.

The measured stress value in CH_30, installed on the bottom edge of the strengthening plate approximately 5'-4 1/2" from the south end of the strengthening plate, is lower than that measured in CH_12 and CH_22 (close to mid span). As mentioned previously, the total stresses in the tie plate and the strengthening plate is a result of superimposing the tensile bending stresses onto the tensile axial stresses. The lower measured value of stress in CH_30 is believed to be due to the fact that bending tensile stresses in the plates is lower near the end of the span (i.e. end of the plate) than at mid span, resulting in total measured stresses being lower in CH_30 than CH_12 or CH_22. Table 5.4 lists a summary of the maximum and minimum stress values experienced by the channels installed on the lower tie plate and the strengthening plate.

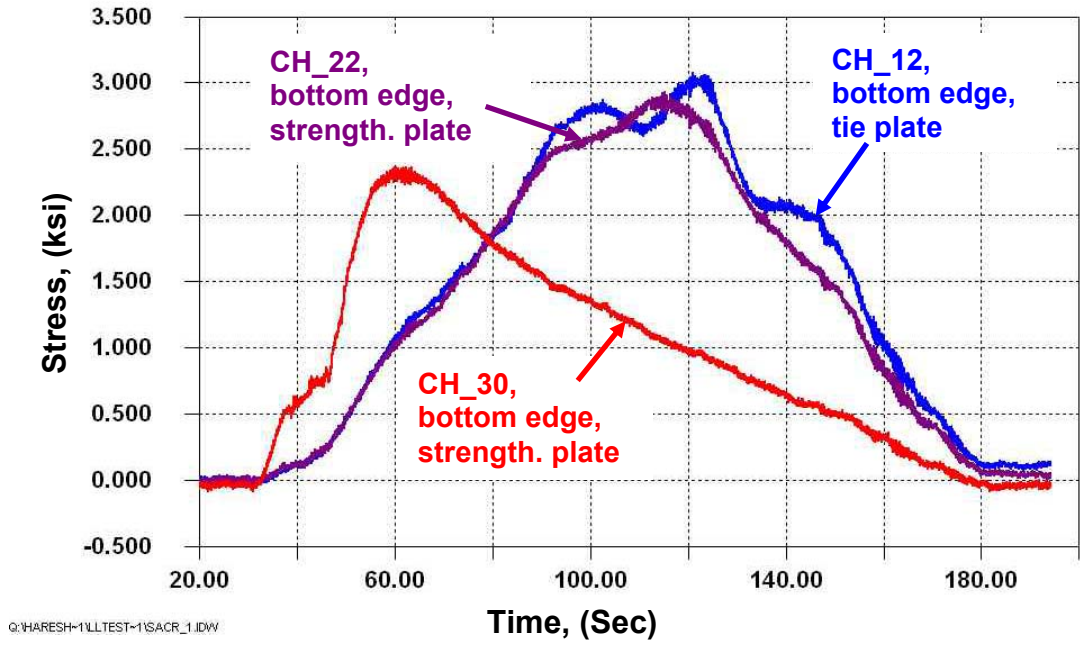

Figure 5.7 – Response of CH_12 and CH_22 installed on the bottom edge of the lower tie plate and the bottom edge of the strengthening plate, respectively, at mid distance between floorbeam 7 and floorbeam 8. Also shown is the response of CH_30 installed on the bottom edge of the lower strengthening plate near the end of the bridge span. The response shown in the figure was during the crossing of the single axle test truck in the crawl test (SACR_1).

Test Designation	CH_11, tie plate, top edge (ksi)		CH_12, tie plate, bottom edge (ksi)	
	σ_{max}	σ_{min}	σ_{max}	σ_{min}
SACR_1.Dat	2.5	0.0	3.0	0.0
SACR_2.Dat	2.4	0.0	2.8	0.0
SACR_3.Dat	2.5	0.0	3.0	0.0
SACR_4.Dat	2.7	0.0	3.0	0.0
SACR_5.Dat	3.0	0.0	3.6	0.0
SACR_6.Dat	2.5	0.0	3.1	0.0
SACR_7.Dat	2.3	0.0	2.7	0.0
TACR_1.Dat	3.4	0.0	4.0	0.0

Test Designation	CH_21, strengthening plate, top edge (ksi)		CH_22, strengthening plate, bottom edge (ksi)	
	σ_{max}	σ_{min}	σ_{max}	σ_{min}
SACR_1.Dat	2.2	0.0	2.9	0.0
SACR_2.Dat	2.0	0.0	2.6	0.0
SACR_3.Dat	2.2	0.0	2.8	0.0
SACR_4.Dat	2.3	0.0	2.9	0.0
SACR_5.Dat	2.6	0.0	3.4	0.0
SACR_6.Dat	2.2	0.0	2.9	0.0
SACR_7.Dat	2.0	0.0	2.6	0.0
TACR_1.Dat	3.0	0.0	3.9	0.0

Test Designation	CH_29, strengthening plate, top edge (ksi)		CH_30, strengthening plate, bottom edge (ksi)	
	σ_{max}	σ_{min}	σ_{max}	σ_{min}
SACR_1.Dat	1.4	0.0	2.3	0.0
SACR_2.Dat	1.2	0.0	2.2	0.0
SACR_3.Dat	1.4	0.0	2.3	0.0
SACR_4.Dat	1.4	0.0	2.4	0.0
SACR_5.Dat	1.6	0.0	2.7	0.0
SACR_6.Dat	1.4	0.0	2.3	0.0
SACR_7.Dat	1.3	0.0	2.1	0.0
TACR_1.Dat	1.9	0.0	3.2	0.0

Table 5.4– Summary of peak measured stresses in CH_11, CH_12 installed on the top and bottom edge of the lower tie plate, respectively, and CH_21, and CH_22 installed on the top and bottom edge of the strengthening plate, respectively, at mid distance between floorbeam 7 and floorbeam 8. Also listed is the response of CH_29 and CH_30 installed on the top and bottom edge of the strengthening plate near the end of the bridge span for the various test truck transverse positions in the crawl tests.

5.7 Stresses in the Lattice Infilling

As previously mentioned, two channels (CH_13 and CH_14) were installed back-to-back on a lattice located near mid span to measure the response of a typical lattice member to moving load. The response of the instrumented lattice member is shown in Figure 5.8. The figure shows that the response in CH_14 installed on the front face of the member (looking west) is higher than the response in CH_13 installed on the back face of the member (looking west). Such observation is an indication of the existence of in-plane axial stresses as well as out-of-plane bending stresses in the instrumented lattice member. The out-of-plane bending stress in the instrumented lattice member suggests that the response of the bridge is similar to that of a beam such that the arch and the tie plates could be considered as the top and bottom flange of the beam, respectively, and the lattice infilling could be considered as the web of the beam. The in-plane and out-of-plane stresses in the member during the crawl test (SACR_1) were calculated and graphed along with the measured stresses as shown in Figure 5.8. A summary of the maximum and minimum stress values experienced by CH_13 and CH_14, installed back-to-back on the front and back face (looking west) of a lattice member located near mid span, in the crawl tests is presented in Table 5.5.

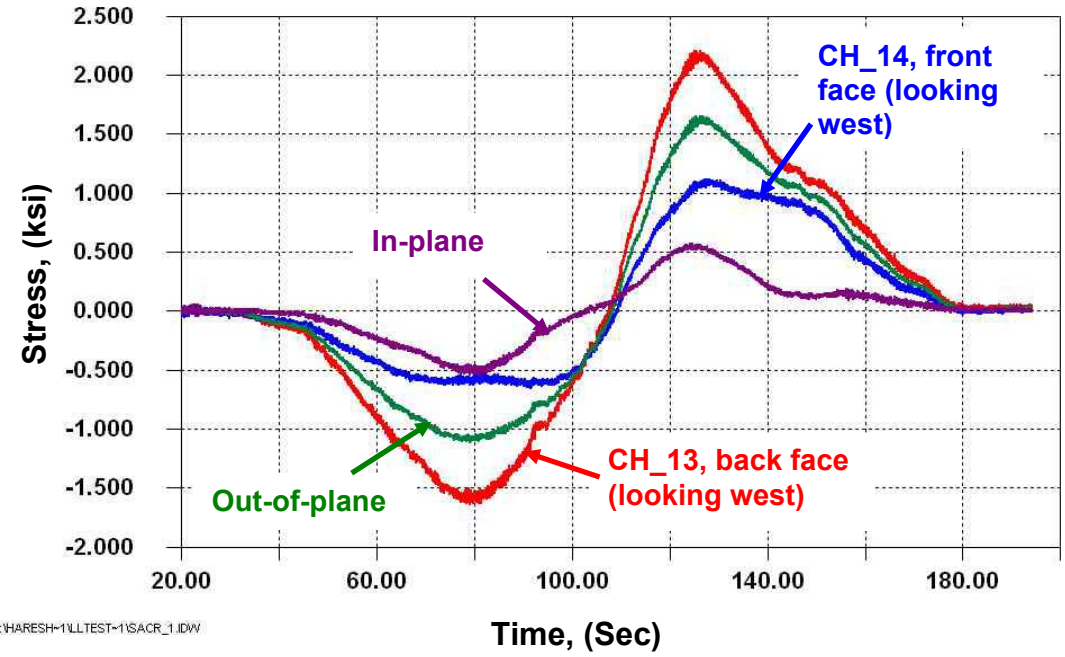

Figure 5.8 – Response of CH_13 and CH_14 installed on the front face and back face (looking west), respectively, of the lattice member located near mid span as the single axle test truck passed over the bridge in the crawl test (SACR_1).

Test Designation	CH_13, lattice, front face (looking west), (ksi)		CH_14, lattice, back face (looking west), (ksi)	
	σ_{max}	σ_{min}	σ_{max}	σ_{min}
SACR_1.Dat	2.2	-1.6	1.0	-0.6
SACR_2.Dat	2.0	-1.5	1.0	-0.6
SACR_3.Dat	2.2	-1.6	1.1	-0.6
SACR_4.Dat	2.3	-1.8	1.1	-0.6
SACR_5.Dat	2.7	-2.1	1.4	-0.7
SACR_6.Dat	2.4	-1.7	1.2	-0.6
SACR_7.Dat	2.0	-1.5	1.0	-0.5
TACR_1.Dat	3.1	-2.3	1.7	-0.9

Table 5.5– Summary of peak measured stresses in CH_13, CH_14 installed on the front and back face (looking west), respectively, of the lattice member located near mid span for the various test truck transverse positions in the crawl tests.

5.8 Stresses in the Floorbeam Connection Plate

Two channels, CH_15 and CH_16, were installed back-to-back on the exterior and interior face (looking west), respectively, of the connection plate used for connecting the lower tie plate to floorbeam 7. The response of the channels to moving load during the crawl test SACR_1 is shown in Figure 5.9. As can be seen in the figure, opposite sign of stresses were observed in the channels (i.e. for a given truck location on the bridge, the stresses are positive in one channel and negative in the other). A summary of the maximum and minimum stress values experienced by CH_15 and CH_16, installed back-to-back on the front and back face of the connection plate connecting the lower tie plate to floorbeam 7, in the crawl tests is presented in Table 5.6. As shown in the table, the positive response in CH_15 is significantly higher than that of CH_16 in all crawl tests. However, the negative response in CH_16 was always higher than that of CH_15 in the same crawl test. Such behavior can not be explained due to the complexity of the system. Understanding the complex behavior of the connection plate detail requires either additional installation of instrumentation at the detail or the development of a detailed finite element model to capture the local response of the detail.

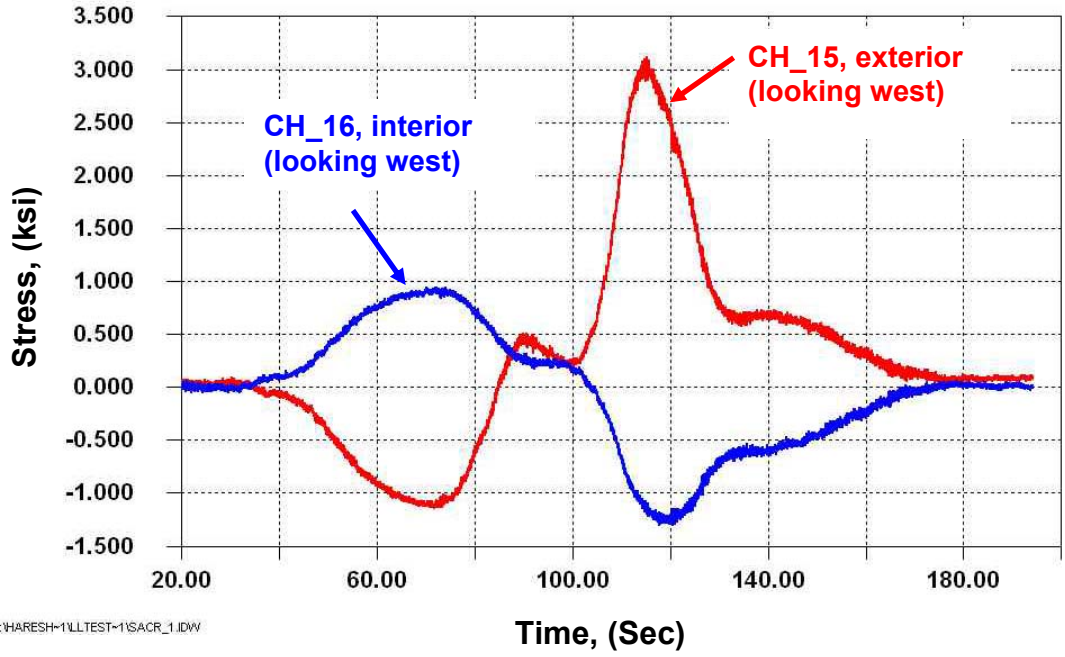

Figure 5.9 – Response of CH_15 and CH_16 installed on the front face and back face (looking west), respectively, of the connection plate used for connecting floorbeam 7 to the lower tie plate, as the single axle test truck passed over the bridge in the crawl test (SACR_1).

Test Designation	CH_15, connection plate, front face (looking west), (ksi)		CH_16, connection plate, back face (looking west), (ksi))	
	σ_{max}	σ_{min}	σ_{max}	σ_{min}
SACR_1.Dat	3.1	-1.1	0.9	-1.3
SACR_2.Dat	2.7	-1.1	0.9	-1.2
SACR_3.Dat	3.1	-1.2	1.0	-1.4
SACR_4.Dat	3.7	-1.3	1.0	-1.5
SACR_5.Dat	5.0	-1.3	1.0	-2.1
SACR_6.Dat	3.7	-1.2	0.9	-1.5
SACR_7.Dat	2.7	-1.1	0.9	-1.2
TACR_1.Dat	4.8	-1.3	1.2	-2.1

Table 5.6– Summary of peak measured stresses in CH_15 and CH_16 installed on the interior and exterior face (looking west), respectively, of the connection plate used for connecting floorbeam 7 to the lower tie plate for the various test truck transverse positions in the crawl tests.

5.9 Stresses in the Floorbeam Connection Rods

Channels CH_17, CH_18, CH_19, and CH_20 were installed on the two connection rods attaching the lower tie plate to floorbeam 8. Channel CH_17 was installed on the connection rod south of the web of floorbeam 8 and CH_18 was installed on the same rod directly behind CH_17. Similarly, Channel CH_19 was installed on the connection rod north of the web of floorbeam 8 and CH_20 was installed directly behind CH_19. As shown in Figure 5.10, positive stresses were measured in CH_17 and CH_18 installed back-to-back on the rod located south of the web of floorbeam 8. The response in CH_18 is higher than that of CH_17 indicating the existence of out-of-plane bending stresses in the rod. Similar behavior was observed in the rod instrumented north of the web of floorbeam 8. A summary of the maximum and minimum stress values experienced by CH_17, CH_18, CH_19, and CH_20 installed back-to-back on the front and back face of the connection rod located south and north of the web of floorbeam 8 in the crawl tests is presented in Table 5.7.

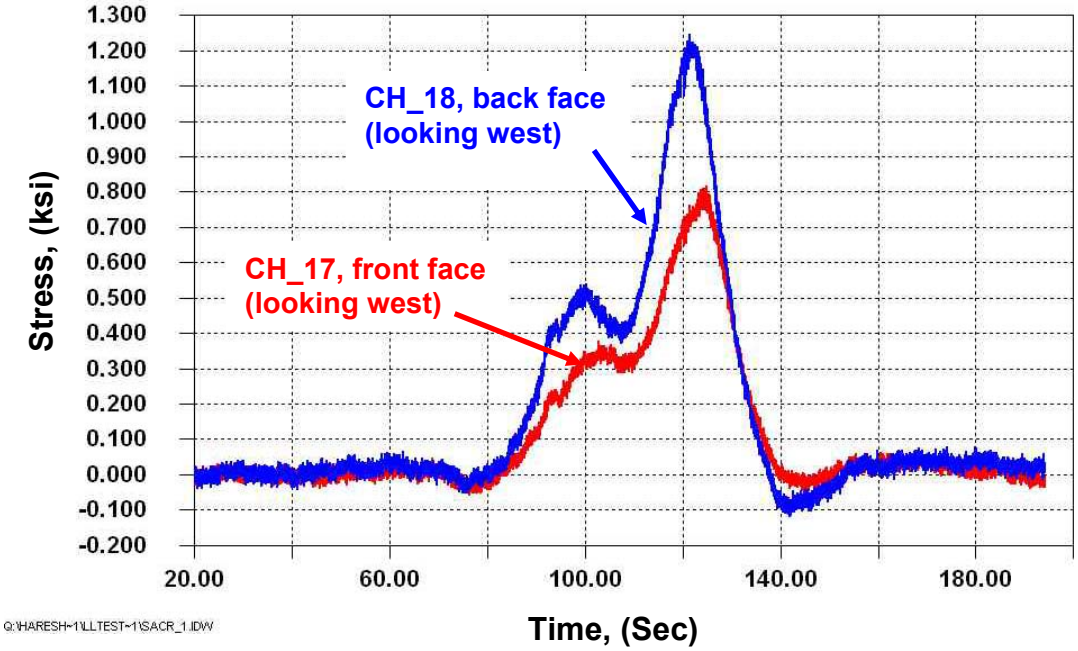

Figure 5.10 – Response of CH_17 and CH_18 installed on the front face and back face (looking west), respectively, of the connection rod used for connection floorbeam 8 to the lower tie plate, as the single axle test truck passed over the bridge in the crawl test (SACR_1).

Test Designation	CH_17, connection rod at FB8 south of FB8 web, front face (looking west), (ksi)		CH_18, connection rod at FB8 south of FB8 web, back face (looking west), (ksi)	
	σ_{max}	σ_{min}	σ_{max}	σ_{min}
SACR_1.Dat	0.8	0.0	1.2	-0.1
SACR_2.Dat	0.7	0.0	1.1	-0.1
SACR_3.Dat	0.8	-0.1	1.2	-0.1
SACR_4.Dat	0.8	0.0	1.4	-0.1
SACR_5.Dat	1.0	0.0	1.5	-0.1
SACR_6.Dat	0.9	0.0	1.3	0.0
SACR_7.Dat	0.7	0.0	1.1	-0.1
TACR_1.Dat	1.2	0.0	1.7	-0.2

Test Designation	CH_19, connection rod at FB8 north of FB8 web, front face (looking west), (ksi)		CH_20, connection rod at FB8 north of FB8 web, back face (looking west), (ksi)	
	σ_{max}	σ_{min}	σ_{max}	σ_{min}
SACR_1.Dat	0.5	-0.2	1.2	-0.1
SACR_2.Dat	0.5	-0.2	1.0	-0.1
SACR_3.Dat	0.5	-0.2	1.1	-0.1
SACR_4.Dat	0.6	-0.2	1.2	-0.1
SACR_5.Dat	0.7	-0.2	1.4	-0.1
SACR_6.Dat	0.6	-0.2	1.2	-0.1
SACR_7.Dat	0.4	-0.2	1.0	-0.1
TACR_1.Dat	0.8	-0.3	1.6	-0.1

Table 5.7– Summary of peak measured stresses in CH_17 and CH_18 installed back-to-back on the front and back face (looking west), respectively, of the connection rod located at floorbeam 8 south of the floorbeam web and CH_19 and CH_20 installed back-to-back on the front and back face (looking west), respectively, of the connection rod located at floorbeam 8 south of the floorbeam for the various test truck transverse positions in the crawl tests.

5.10 Stresses in the Bottom Flange of Stringers

As previously mentioned, CH_26, CH_27, and CH_28 were installed on the bottom face of the bottom flange at centerline of the flange on stringers S11, S10, and S9, respectively, at mid distance between floorbeam 7 and floorbeam 8. The response of the channels to moving load in the controlled crawl test (SACR_1) can be seen in Figure 5.11. As shown in the figure, positive stresses were in the bottom flange in all three channels. Also shown in the figure, is the peak response caused by the front axle of the single test truck being located directly over the channels. In such case, the response was higher in CH_28 flowed by CH_27 and finally CH_26. When the rear axle was located directly over the channels, the stresses were higher in CH_ 27 followed by CH_28 and finally CH_26. It is unclear as to why the stresses were highest in CH_28 as the front axle was directly located over the channel, while it was highest in CH_27 when the rear axle was directly located over the channel. It is possible that such behavior is due to slight change in the transverse position of the truck as it was crossing the bridge.

In general, the response of the channels installed on the bottom flange of the stringers was very sensitive to the transverse location of the test truck(s) in the crawl tests. The sensitivity of the instrumented locations to the transverse position of the testing truck is shown in Table 5.8. The table shows that the response of CH_26 to the passage of the single axle truck (lighter truck) during the crawl test (SACR_5) is almost two times higher than the response of the same channel to the passage of the tandem axle truck (heavier truck) during the crawl test (TACR_1). It is important to mention that with the exception of the channels installed on the bottom flange of the stringers, the response of any given channel to the passage of the tandem axle truck in the crawl test (TACR_1) was higher than the response during the passage of the single axle truck in the seven crawl tests (SACR_1 through SACR_7). A summary of the maximum and minimum stress values experienced by CH_26, CH_27, and CH_28 installed on the bottom face of the bottom flange of stringers S11, S10, and S9, respectively, in the crawl tests is presented in Table 5.8.

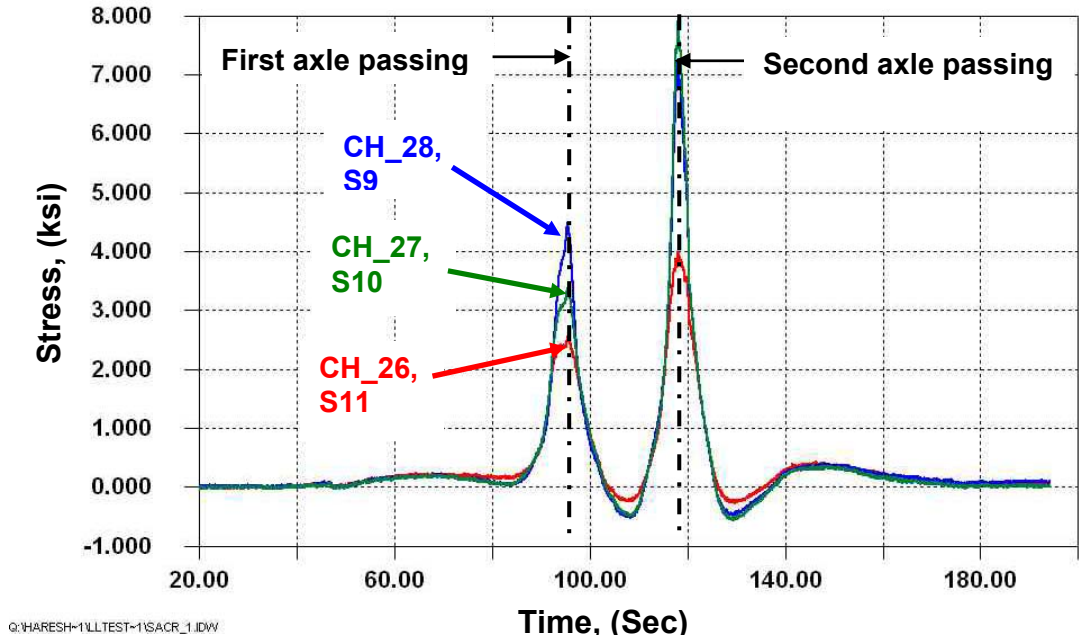

Figure 5.11 – Response of CH_26, CH_27, and CH_28 installed on the bottom face of the bottom flange at centerline of the flange of stringers S11, S10, and S9, respectively, at mid distance between floorbeam 7 and floorbeam 8 as the single axle test truck passed over the bridge in the crawl test (SACR_1).

Test Designation	CH_26, centerline of bottom flange of S11, between FB8 & FB7, (ksi)		CH_27, centerline of bottom flange of S10, between FB8 & FB7, (ksi)		CH_28, centerline of bottom flange of S9, between FB8 & FB7, (ksi)	
	σ_{max}	σ_{min}	σ_{max}	σ_{min}	σ_{max}	σ_{min}
SACR_1.Dat	3.9	-0.3	7.2	-0.5	7.9	-0.6
SACR_2.Dat	2.9	-0.3	5.7	-0.6	7.8	-0.6
SACR_3.Dat	4.4	-0.3	7.4	-0.6	7.4	-0.5
SACR_4.Dat	5.2	-0.3	7.6	-0.6	6.4	-0.5
SACR_5.Dat	8.0	-0.4	5.8	-0.6	3.9	-0.5
SACR_6.Dat	5.5	-0.3	7.8	-0.6	6.5	-0.6
SACR_7.Dat	3.0	-0.3	6.0	-0.6	7.9	-0.5
TACR_1.Dat	4.4	-0.4	6.4	-0.7	5.4	-0.7

Table 5.8– Summary of peak measured stresses in CH_26, CH_27, and CH_28 installed on the bottom face of the bottom flange at centerline of the flange of stringers S11, S10, and S9, respectively, at mid distance between floorbeam 7 and floorbeam 8 for the various test truck transverse positions in the crawl tests.

5.11 Stresses in the Diagonal Tension Bar

Channel CH_31 was installed on the east face of the bar, while CH_32 was installed on the west face. The gages were installed on the east diagonal tension bar at a diagonal distance of approximately 11'-6" away from the end of the bar at floorbeam 8. The bar ties the east arch Z-Bar near floorbeam 2 to the bottom end of the vertical T-shape member at floorbeam 8. The response of the two gages during the controlled load test (SACR_1) is shown in Figure 5.12. The response of CH_31 is shown to be positive during the entire time of the crawl test (SACR_1), while the response of CH_32 is shown to be negative for approximately 50 seconds of the test followed by positive response during the remainder of the test. As shown in the figure, during the first 50 seconds of the test, out-of-plane bending of the rod was the dominate behavior. After which, the behavior of the rod was mainly axial tension. A summary of the maximum and minimum stress values experienced by CH_31 and CH_32 installed on the east and west face, respectively, of the east diagonal tension bar at a diagonal distance of approximately 11'-6" away from the end of the bar at floorbeam 8 is presented in Table 5.9.

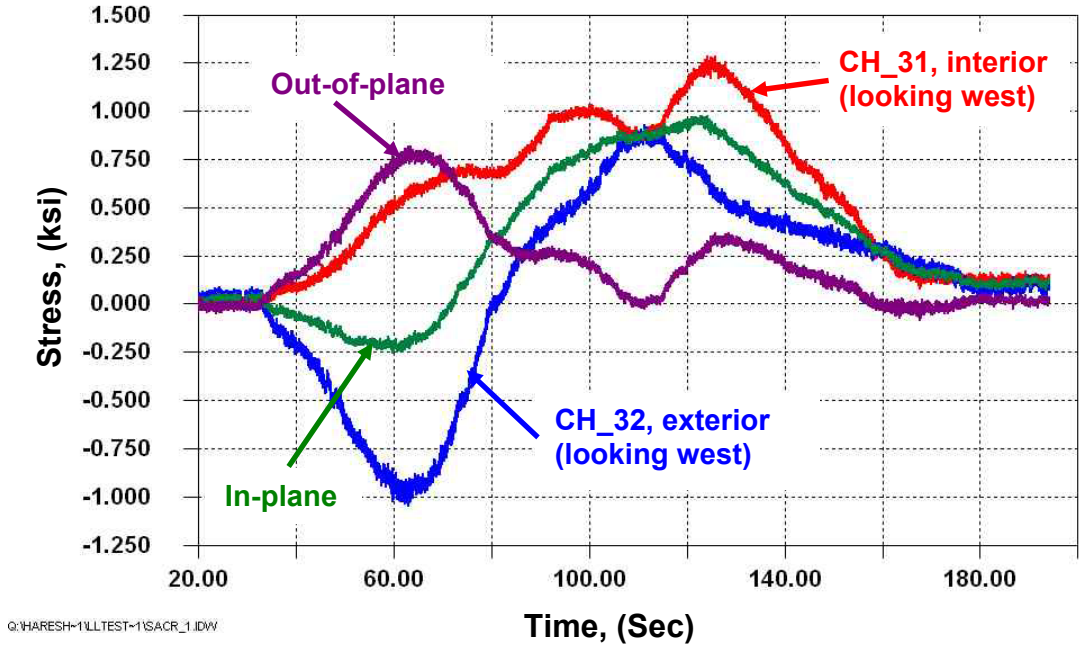

Figure 5.12 – Response of CH_31 and CH_32 installed on the east and west face, respectively, of the east diagonal tension bar at a diagonal distance of approximately 11'-6" away from the end of the bar at floorbeam 8 as the single axle test truck passed over the bridge in the crawl test (SACR_1).

Test Designation	CH_31, diagonal tension bar, front face (looking west), (ksi)		CH_32, diagonal tension bar, back face (looking west), (ksi)	
	σ_{max}	σ_{min}	σ_{max}	σ_{min}
SACR_1.Dat	1.3	0.0	0.9	-1.0
SACR_2.Dat	1.1	0.0	0.8	-0.9
SACR_3.Dat	1.1	0.0	0.8	-0.9
SACR_4.Dat	1.3	0.0	0.9	-1.2
SACR_5.Dat	1.4	0.0	0.9	-1.3
SACR_6.Dat	1.2	0.0	0.9	-1.1
SACR_7.Dat	1.1	0.0	0.8	-1.0
TACR_1.Dat	1.5	-0.1	1.1	-1.6

Table 5.9– Summary of peak measured stresses in CH_31 and CH_32 installed on the east and west face, respectively, of the east diagonal tension bar at a diagonal distance of approximately 11'-6" away from the end of the bar at floorbeam 8 for the various test truck transverse positions in the crawl tests

5.12 Dynamic Response

To gain a feel for the magnitude of dynamic amplification of stresses in the bridge, two dynamic load tests were conducted with the single axle test truck traveling north in the first test at a speed of approximately 15 mph and traveling south in the second test at a speed of 17 mph. Figure 5.13 contains a stress time-history for the east Z-Bar located on the east side of the bridge, during a dynamic test with the single axle test truck traveling north with a speed of 15 mph. This figure can be compared with Figure 5.1 above, which shows a similar stress history for the crawl test (SACR_1). Also comparing both figures shows that more vibration was introduced in the east Z-Bar on the east side of the bridge during the dynamic test.

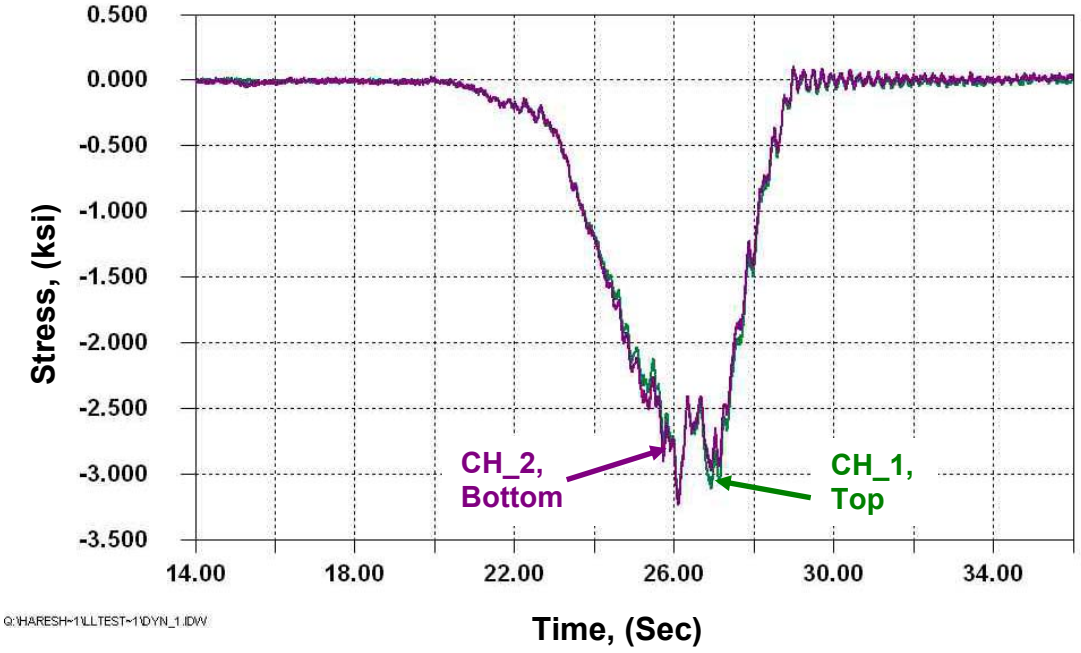

Figure 5.13 – Response of CH_1 and CH_2 installed on the top and bottom face, respectively, of the west Z-Bar on the east side of the bridge, 1 inch from the edge of the bar and approximately 3 inches south of floorbeam 8, as the single axle test truck passed over the bridge in the dynamic test (DYN_1)

A summary of the peak tension and compression stresses for both the crawl test (SACR_2) and the dynamic test (DYN_1) is shown in Table 5.10. Also listed in the table is the dynamic amplification factor, which is taken as the ratio between both tests. The reason for choosing the crawl test (SACR_2) to be compared with the dynamic test (DYN_1) and the calculation of the dynamic amplification factor is because the response of the channels installed on the bottom flange of the stringers (CH_26, CH_27, and CH_28) is almost identical in both tests. The identical response of these channels in both tests suggests that the transverse location of the test truck in both tests was very similar, since the response in these particular channels is highly sensitive to the transverse

location of the test truck (Section 5.10). The peak stress values obtained during the dynamic controlled test (DYN_2) is also listed in the table. However, no dynamic amplification factor was calculated based on that test since the response of CH_26, CH_27, and CH_28 during the controlled test (DYN_2) did not correlate well with the response of the same channels in any of the crawl tests.

With the exception of CH_9, the dynamic amplification factor of stresses at all locations varied between 1.0 and 1.3. The summation of the tensile stress ratios listed in Table 5.10 is 32.9 and the average ratio is 1.03. If the dynamic amplification factor calculated for CH_9 is excluded, then the summation of the tensile dynamic multiplication factor is 32.4 and the average value is 1.05. The summation of the compressive dynamic multiplication factor is 33.5 and the average value is 1.05. The typical ratio of 1.05 indicates that the bridge experiences little dynamic amplification factor at low speed (15 mph). It is important to mention that the calculated dynamic amplification factor of 1.05 is based on limited data (one controlled dynamic test at 15 mph). Higher travel speed (25 mph – 35 mph) could increase the dynamic amplification factor. However, there was no data collected at these speeds. The possibility of higher dynamic amplification factors at higher speeds is highly unlikely when vehicles are traveling south since the orientation of the south approach to the bridge should keep the speed of most vehicles down in the 15 mph range.

	Channel No.	Crawl Test (SACR_2)		Dynamic Test (DYN_1)		Dynamic Test (DYN_2)		*(DYN_1/SACR_2)*	
		Tens. (ksi)	Compr. (ksi)	Tens. (ksi)	Compr. (ksi)	Tens. (ksi)	Compr. (ksi)	Tens.	Compr.
Z_BAR Arches	CH_1	0.1	-3.0	0.1	-3.2	0.1	-3.4	1.0	1.1
	CH_2	0.1	-3.0	0.1	-3.2	0.1	-3.4	1.0	1.1
	CH_3	0.0	-4.2	0.0	-4.6	0.0	-4.5	1.0	1.1
	CH_4	0.0	-3.6	0.0	-3.9	0.0	-3.8	1.0	1.1
	CH_24	0.1	-3.5	0.1	-3.8	0.1	-3.5	1.0	1.1
	CH_25	0.1	-3.7	0.1	-4.0	0.1	-3.5	1.0	1.1
Floorbeam Flanges	CH_5	0.0	-2.4	0.0	-2.6	0.1	-2.5	1.0	1.1
	CH_6	1.7	-0.1	1.8	-0.1	1.7	-0.1	1.1	1.0
	CH_9	0.17	-3.0	0.11	-3.3	0.11	-3.0	0.64	1.1
	CH_10	4.4	-0.1	4.8	-0.1	4.2	-0.2	1.1	1.0
Diag. & Vertical Strut	CH_7	5.2	0.0	5.9	-0.1	5.6	-0.1	1.1	1.0
	CH_8	4.9	0.0	5.4	-0.1	5.2	-0.1	1.1	1.0
	CH_23	0.1	-1.1	0.1	-1.2	0.1	-1.1	1.0	1.1
Lower Plate & Strength. Plate	CH_11	2.4	0.0	2.4	0.0	2.6	0.0	1.0	1.0
	CH_12	2.8	0.0	2.8	0.0	2.9	0.0	1.0	1.0
	CH_21	2.0	0.0	2.0	0.0	2.0	0.0	1.0	1.0
	CH_22	2.6	0.0	2.7	0.0	2.7	0.0	1.0	1.0
	CH_29	1.2	0.0	1.2	0.0	1.3	0.0	1.0	1.0
	CH_30	2.2	0.0	2.1	0.0	2.3	0.0	1.0	1.0
Lattice Infilling	CH_13	2.0	-1.5	2.1	-1.5	1.9	-2.2	1.0	1.0
	CH_14	1.0	-0.6	1.1	-0.7	1.1	-0.8	1.0	1.0
Connection Plate	CH_15	2.7	-1.1	3.1	-1.1	2.9	-1.5	1.1	1.0
	CH_16	0.9	-1.2	1.0	-1.4	1.2	-1.2	1.1	1.2
Floorbeam Connection Rods	CH_17	0.7	0.0	0.8	0.0	0.8	0.0	1.1	1.0
	CH_18	1.1	-0.1	1.2	-0.1	1.2	-0.1	1.1	1.0
	CH_19	0.5	-0.2	0.6	-0.2	0.5	-0.2	1.2	1.0
	CH_20	1.0	-0.1	1.0	-0.1	1.0	-0.1	1.0	1.0
Bottom Flange of Stringer	CH_26	2.9	-0.3	3.0	-0.4	3.8	-0.6	1.0	1.3
	CH_27	5.7	-0.6	5.8	-0.6	7.0	-0.8	1.0	1.0
	CH_28	7.8	-0.6	7.6	-0.6	7.7	-0.8	1.0	1.0
Diag. Tension Bar	CH_31	1.1	0.0	1.2	0.0	1.2	0.0	1.1	1.0
	CH_32	0.8	-0.9	1.0	-1.0	0.9	-1.1	1.3	1.1

Table 5.10 – Summary of peak tension stress and compression stress for the crawl test (SACR_2) and the dynamic tests (DYN_1) and (DYN_2).
Also shown are the stress ratios = (DYN_1/SACR2)

6.0 Short-term Monitoring

The short-term monitoring of the tied arch was conducted from May 18, 2005 until May 21, 2005 for total of approximately 3.2 days. Stress time-history data were recorded in all 32 channels when a predefined trigger value was exceeded in a particular channel. In addition to the triggered events, stress-range histograms of 10 selected channels were generated based on a review of the controlled load test data.

6.1 Results of Short-term Monitoring

The rainflow cycle counting method was used to develop the stress-range histograms for the ten selected channels. Although the method is typically used in fatigue evaluation of structures (which is not the intention of this project), it was felt that producing the histograms should give a good indication to the response of the channels to random traffic. The stress time-history data recorded during the 3.2 days of monitoring was viewed and showed no sign of extreme events in any of the 32 channels. In fact, the highest stress value recorded in each channel during the monitoring period was less than the maximum recorded by the channels during the controlled crawl load tests using the single axle truck. For example, the highest recorded compressive stress value in CH_1 during the controlled crawl tests was 4.1 ksi in the crawl test (SACR_5). The highest compressive stress value recorded, however, by the same channel during the 3.2 days monitoring was 2.2 ksi (Figure 6.1 and Figure 6.2). A discussion of the results of the Short-term monitoring of the ten selected channels is presented below.

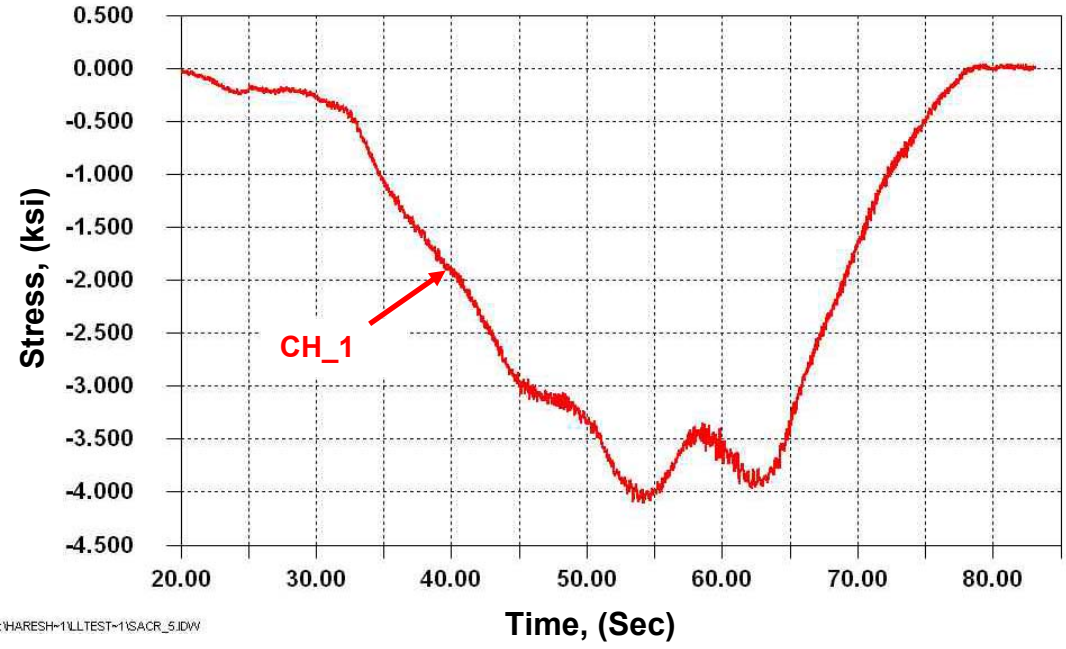

Figure 6.1 – Response of CH_1 installed on the top face of the west Z-Bar on the east side of the bridge, 1 inch from the edge of the bar and approximately 3 inches south of floorbeam 8, as the single axle test truck passed over the bridge in the crawl test (SACR_5)

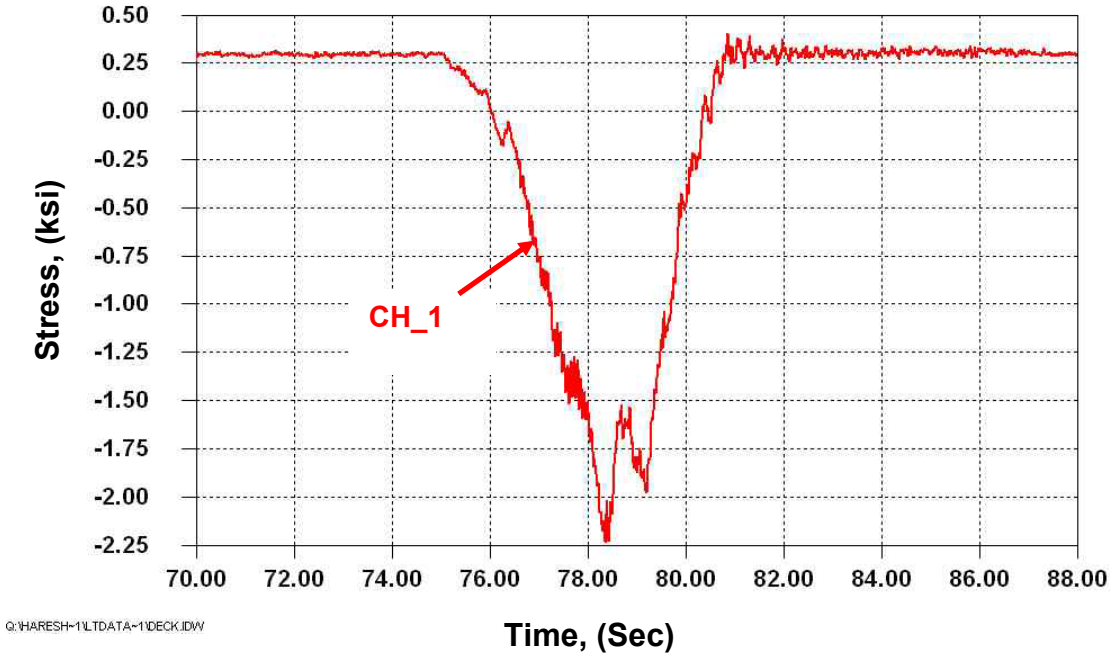

Figure 6.2 – Time history response of CH_1 installed on the top face of the west Z-Bar on the east side of the bridge, 1 inch from the edge of the bar and approximately 3 inches south of floorbeam 8, during the long-term random monitoring of the channel. The response shown took place on May 18, 2005 at 3:24 PM

6.2 Stress-Range Histograms

6.2.1 Stresses in Floorbeam Flanges

As previously discussed, CH_6 and CH_10 were installed on the bottom flanges of floorbeam 8 and floorbeam 7, respectively. The histograms were divided in 0.5 ksi bins. The stress-range histogram for both channels is shown in Figure 6.3. The maximum stress range recorded by CH_6 is within the bin of 1.0 ksi – 1.5 ksi. An average maximum stress-range value of 1.25 ksi could therefore be assumed. For CH_10, the average maximum stress-range value recorded by CH_10 during the monitoring period is 3.25 ksi.

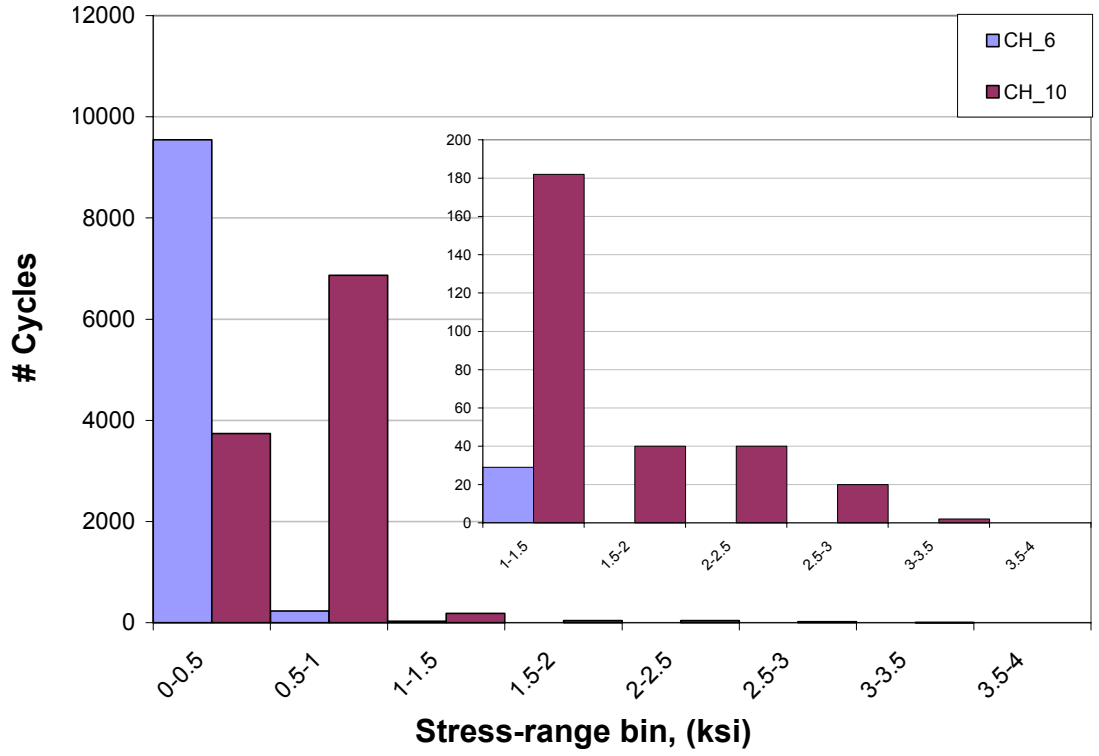

Figure 6.3 – Stress range histogram for CH_6 installed on the bottom flange of floorbeam 8 and CH_10 installed on the bottom flange of floorbeam 7

6.2.2 Stresses in the Diagonal Strut of the Queen Post

Channels CH_7 was installed on the bottom face of the diagonal strut attached to the bottom flange of floorbeam 8. Figure 6.4 presents the stress-range histogram of the channel. The average maximum stress range recorded by CH_6 is 3.75 ksi.

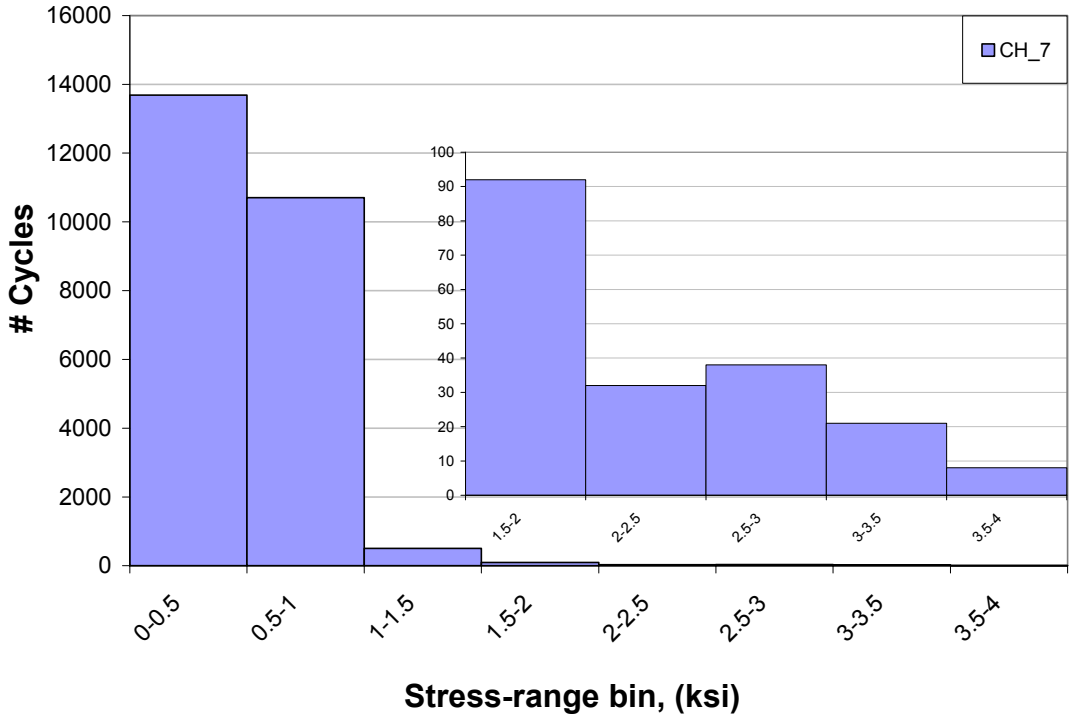

Figure 6.4 – Stress range histogram for CH_7 installed on the bottom face at mid length of the diagonal strut attached to floorbeam 8

6.2.3 Stresses in the Lower and Strengthening Tie Plates

As mentioned in Chapter 4, six channels were installed on the lower and strengthening tie plates to measure their response to moving load. From the six channels installed, two channels were selected for the short-term monitoring, namely CH_12 and CH_22. Channels CH_12 and CH_22 were installed on the bottom edge of the lower tie plate and strengthening plate, respectively, at mid distance between floorbeam 7 and floorbeam 8. Figure 6.5 shows the stress-range histogram of both channels. The average maximum stress range recorded by both channels is 2.25 ksi.

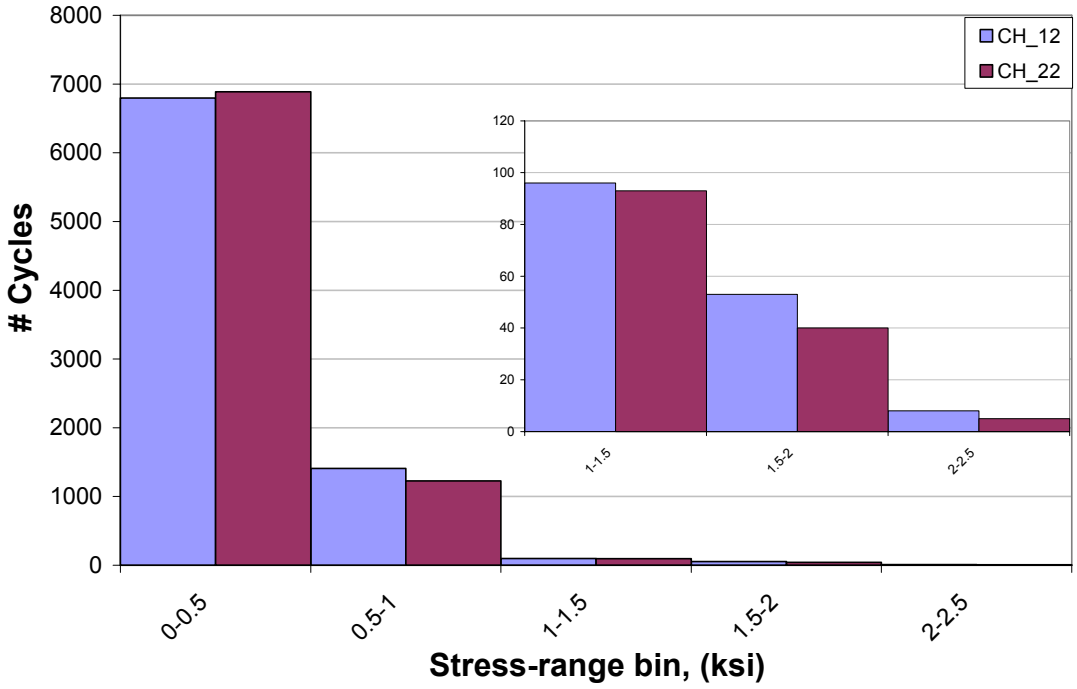

Figure 6.5 – Stress range histogram for CH_12 and CH_22 installed on the bottom edge of the lower tie plate and strengthening plate, respectively, at mid distance between floorbeam 7 and floorbeam 8.

6.2.4 Stresses in the Lattice Infilling

Channels CH_13 and CH_14, installed back-to-back on the front and back face of a lattice member located near mid span. Channel CH_13 was selected for the short-term monitoring. Figure 6.6 shows the stress-range histogram of the channel. As can be seen in the figure, the maximum stress range recorded by the channel falls in the bin of 2.5 ksi – 3.0 ksi, with and average maximum stress of 2.75 ksi.

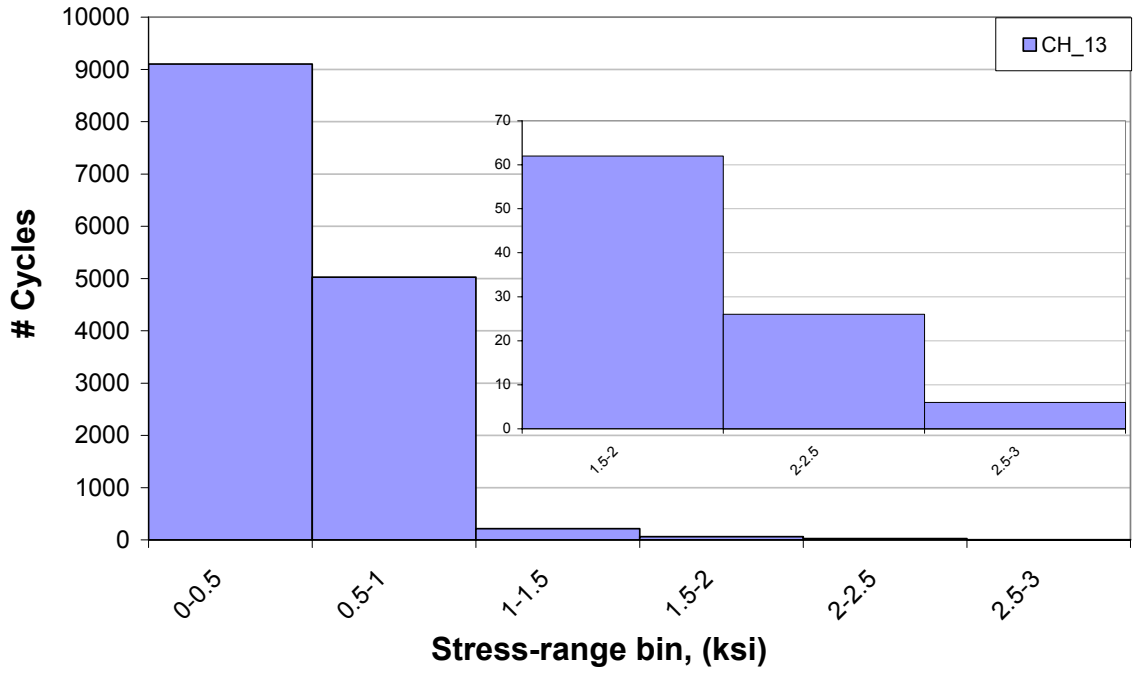

Figure 6.6 – Stress range histogram for CH_13 and CH_14 installed back-to-back on the front and back face of a lattice member located near mid span

6.2.5 Stresses in the Floorbeam Connection Plate

Channels CH_15 and CH_16, were installed back-to-back on the front and back face, respectively, of the connection plate used for connecting the lower tie plate to floorbeam 7. The stress-range histogram was developed for CH_15 and is shown in Figure 6.7. As shown in the figure, the maximum stress range recorded by the channel falls in the bin of 4.0 ksi – 4.5 ksi, with and average maximum stress of 4.25 ksi.

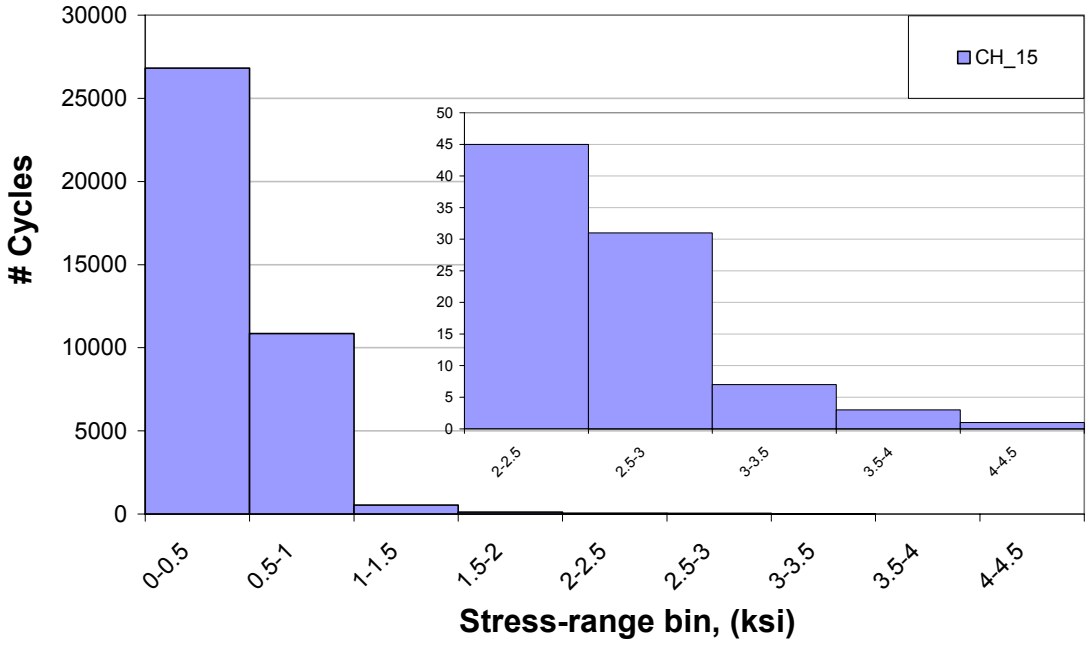

Figure 6.7 – Stress range histogram for CH_15 installed on the front face of the connection plate used for connecting the lower tie plate to floorbeam 7

6.2.6 Stresses in the Floorbeam Connection Rods

As mentioned previously, four channels were installed on the connection rods located at floorbeam 8. Specifically, channel CH_17 was installed on the front face of the connection rod south of the web of floorbeam 8 and CH_18 was installed on the same rod directly behind CH_17. Similarly, Channel CH_19 was installed on the connection rod north of the web of floorbeam 8 and CH_20 was installed directly behind CH_19. Two channels (CH_18 and CH_20) were chosen for the short-term monitoring. The stress-range histogram of both channels is shown in Figure 6.8. An average maximum stress of 1.25 ksi and 0.75 ksi was recorded by CH_18 and CH_20, respectively, during the monitoring period.

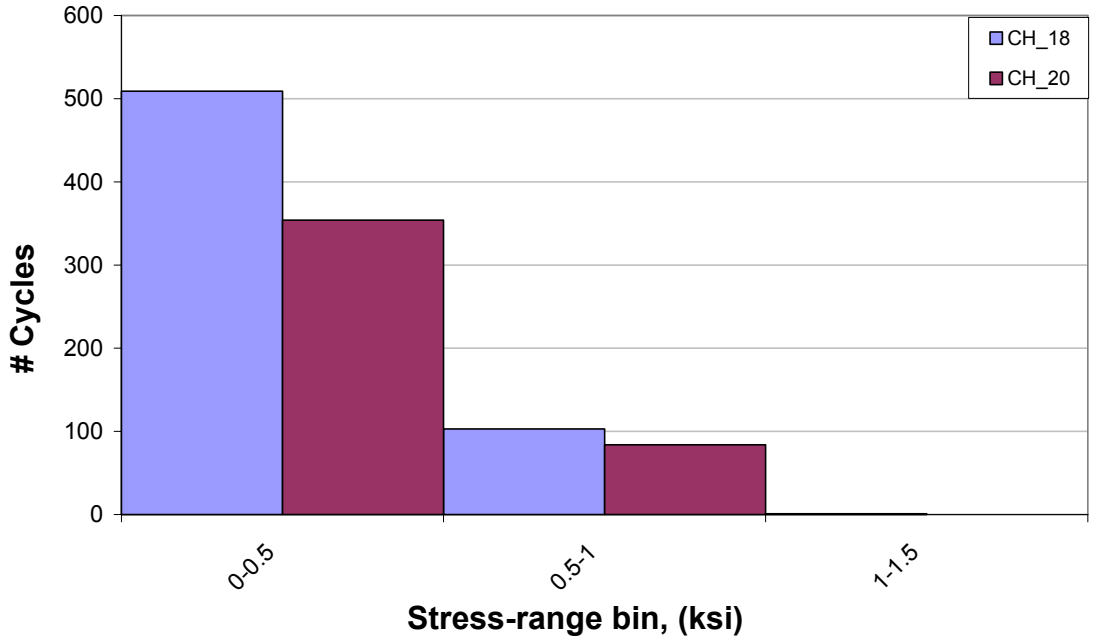

Figure 6.8 – Stress range histogram for CH_18 and CH_20 installed on the connection rods located at floorbeam 8

6.2.7 Stresses in the Diagonal Tension Bar

A stress-range histogram was developed for CH_32 installed on the east diagonal tension bar at a diagonal distance of approximately 11'-6" away from the end of the bar at floorbeam 8. The histogram (Figure 6.9) shows that the average maximum stress range value measure during monitoring was 1.75 ksi.

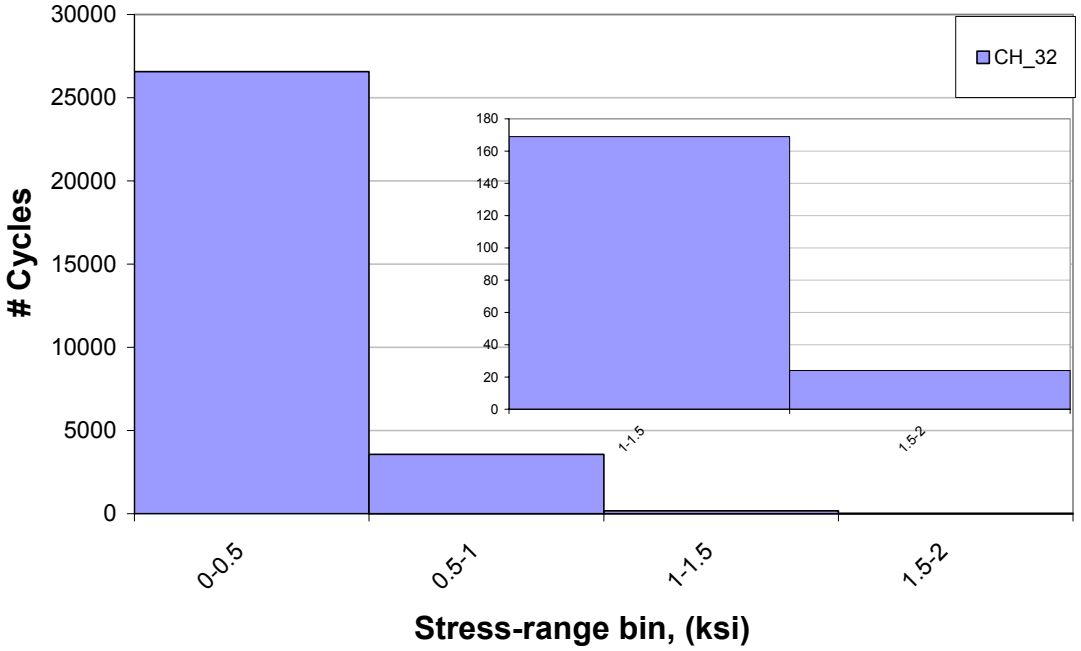

Figure 6.9 – Stress range histogram for CH_32 installed on the east diagonal tension bar at a diagonal distance of approximately 11'-6" away from the end of the bar at floorbeam 8

7.0 Summary and Conclusion

The following section provides a summary of the project and the results of the controlled load testing and short-term monitoring conducted on the Hares Hill Road Bridge in Chester County, Pennsylvania.

Instrumentation Plan

1. The instrumentation plans were developed by ATLSS researchers, with aid from engineers at Mackin Engineering Company.

2. Instrumentation was installed at key locations to determine the local response of the instrumented locations as well as the overall response of the bridge.

3. The instrumented locations included the Z-Bar arches, floorbeam flanges, diagonal and vertical strut of the queen post, lower and strengthening tie plates, lattice infilling, floorbeam connection plate, floorbeam connection rod, bottom flange of stringers, and diagonal tension bar.

Controlled Load Testing

1. The bridge responded as a beam such that the arch and the tie plates could be considered as the top and bottom flange of a beam, respectively, and the lattice infilling could be considered as the web of the beam. The bridge also responded as a tied arch bridge.

2. The results of the controlled load tests did not show any sign of unexpected behavior except at the floorbeam connection plate, which was subject to more bending.

3. With the exception of the channels installed on the bottom flange of the stringers, the response of any given channel to the passage of the tandem axle truck in the crawl test (TACR_1) was higher than the response during the passage of the single axle truck in the seven crawl tests (SACR_1 through SACR_7)

4. The response of the channels installed on the bottom flange of the stringers was very sensitive to the transverse location of the test truck.

5. With the exception of CH_9, the dynamic amplification factor of stresses at all locations varied between 1.0 and 1.3.

6. The calculated dynamic amplification factors are based on one dynamic test (DYN_1) where the single axle test truck was traveling across the bridge at a speed of approximately 15 mph.

Short-Term Monitoring

1. The bridge was monitored under random traffic for a period of 3.2 days. Additional monitoring for one month or more would be required to fully characterize the random live load spectrum.

2. Time-history data collected during the monitoring period showed no sign of extreme events in any of the 32 channels.

3. The highest stress value recorded in each channel during the monitoring period was less than the maximum recorded by the channels during the controlled crawl load tests using the single axle truck.

4. Stress-range histograms were developed for 10 channels selected on the bridge. Although the stress-range histograms are typically developed for fatigue evaluation, which is not the intention of this study, the histograms gave good indication of the response of the channels to random traffic.

Appendix A

Instrumentation Plans

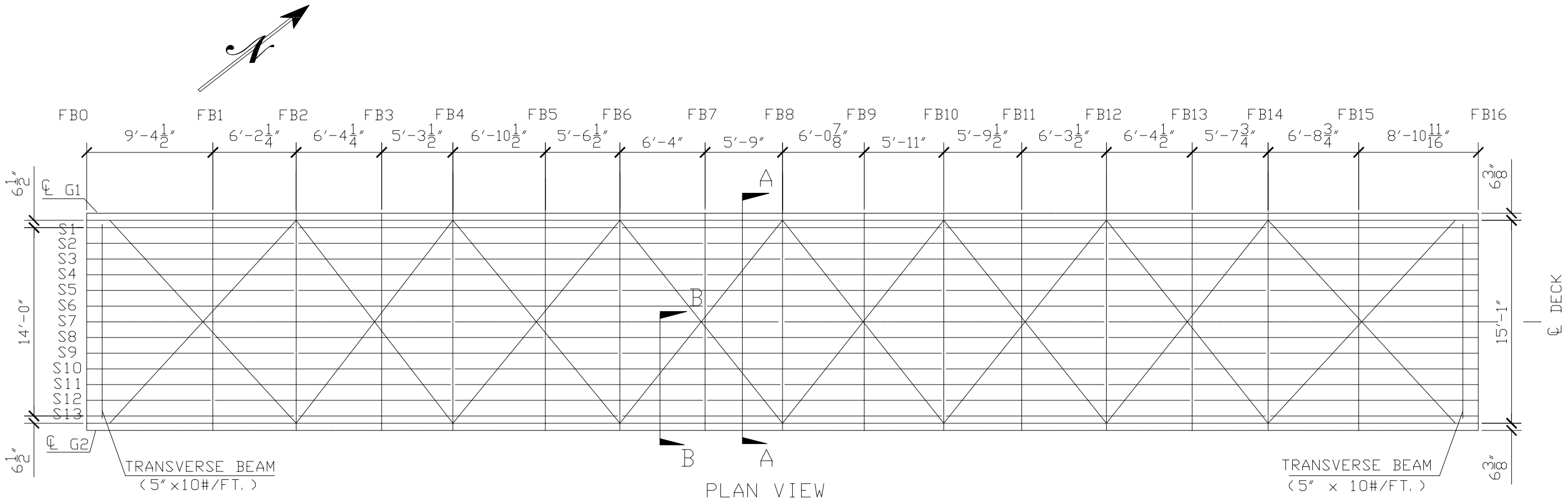

PLAN VIEW
SCALE: 1/8″ = 1′

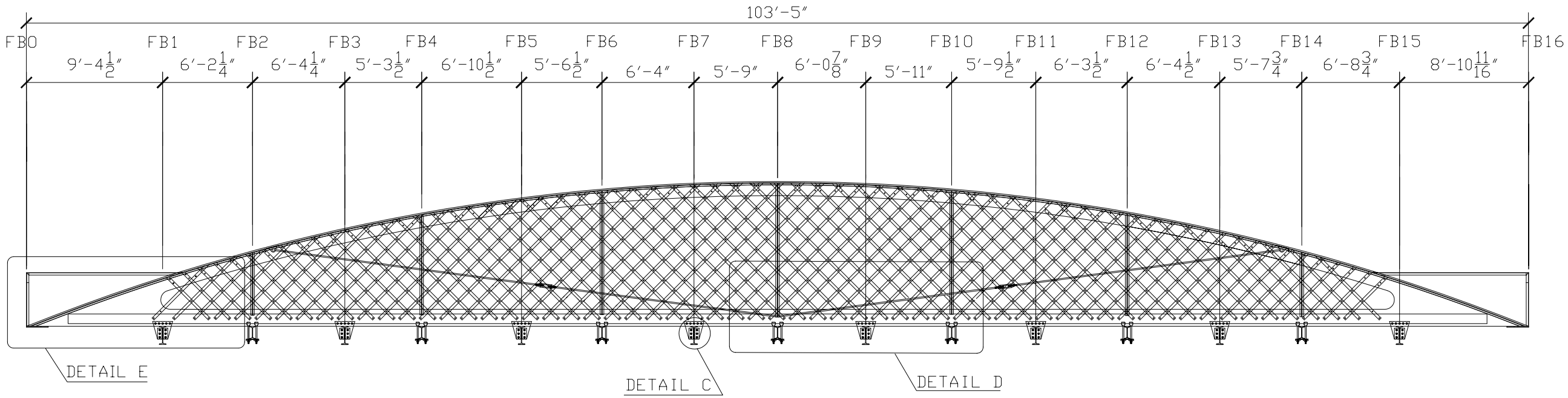

ELEVATION
SCALE: 1/8″ = 1′

ATLSS
ADVANCED TECHNOLOGY FOR LARGE STRUCTURAL SYSTEMS
117 ATLSS Drive
Lehigh University
Bethlehem, PA 18015
610-758-3535 FAX 610-758-6842

PROJECT:

HARES HILL BRIDGE, CHESTER COUNTY, PA

SHEET NOTES:

NO.	DESCRIPTION	DATE	BY
1	INITIAL SUBMITTAL	5/4/05	HNM

DESIGNED BY:	RJC, HNM
DRAWN BY:	HNM
CHECKED BY:	RJC
SCALE:	1/8" = 1'-0"
DATE:	5/18/05
PROJECT NO.:	AT149.1
SHEET TITLE:	

SHEET TITLE

SHEET NO.:

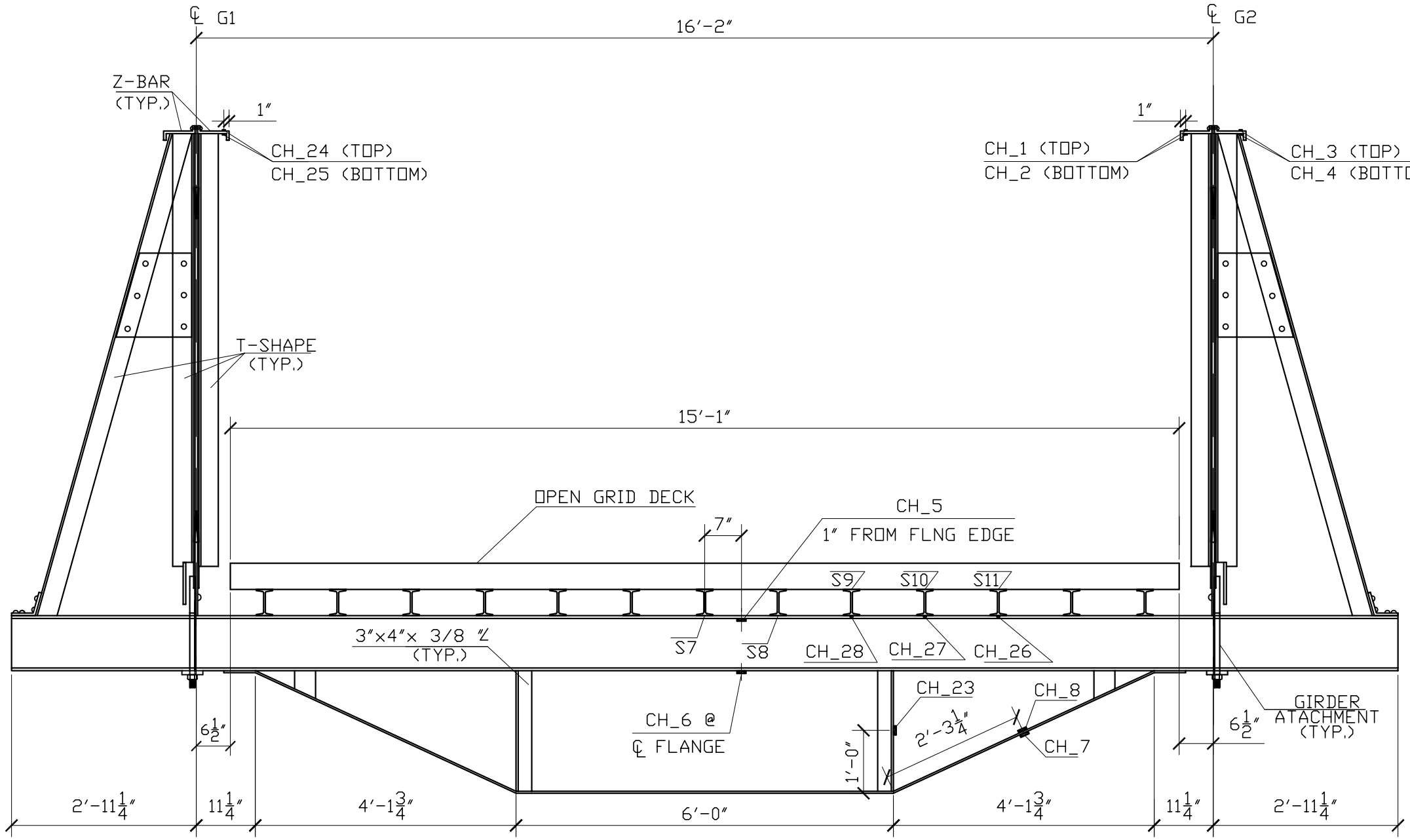

SECTION A-A
VIEW LOOKING NORTH
SCALE: 1/2″ = 1′

NOTE:
CH_1 THROUGH CH_4 ARE 3″ SOUTH OF THE CENTERLINE OF FLOORBEAM 8

NOTE:
CH_26, CH_27, AND CH_28 ARE HALF WAY BETWEEN FB 7 AND FB 8

ATLSS
ADVANCED TECHNOLOGY FOR LARGE STRUCTURAL SYSTEMS
117 ATLSS Drive
Lehigh University
Bethlehem, PA 18015
610-758-3535 FAX 610-758-6842

PROJECT:

HARES HILL BRIDGE, CHESTER COUNTY, PA

SHEET NOTES:

NO.	DESCRIPTION	DATE	BY
1	INITIAL SUBMITTAL	5/4/05	

DESIGNED BY:	RJC AND HNM
DRAWN BY:	HNM
CHECKED BY:	RJC
SCALE:	1/2" = 1'-0"
DATE:	5/18/05
PROJECT NO.:	AT149.1

SHEET TITLE:

SHEET TITLE

SHEET NO.:

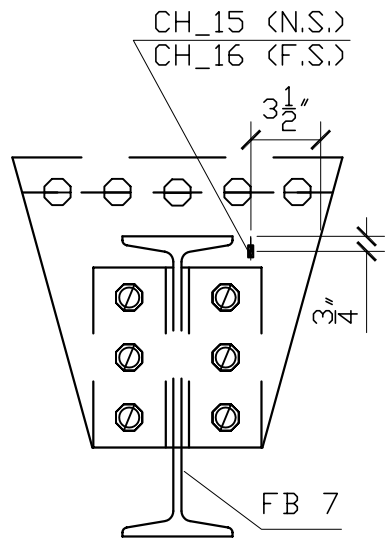

DETAIL C AT FB 7
VIEW LOOKING WEST

SCALE: 1 1/4" = 1'

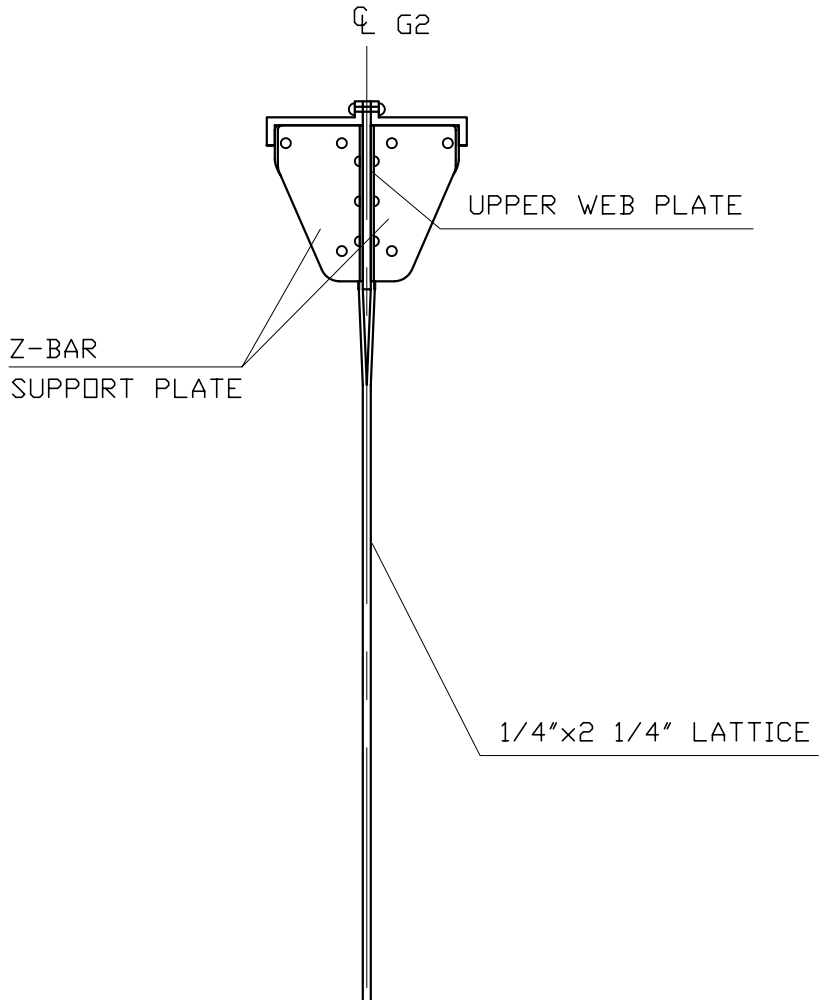

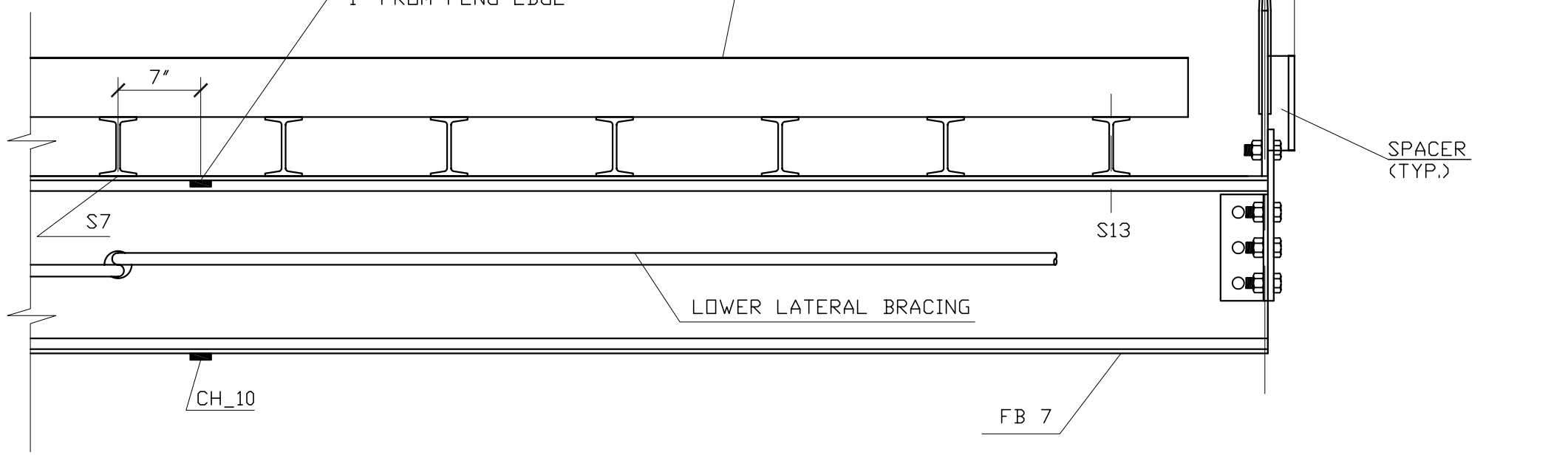

SECTION B-B
VIEW LOOKING NORTH

SCALE: 1" = 1'

ATLSS

117 ATLSS Drive
Lehigh University
Bethlehem, PA 18015
610-758-3535 FAX 610-758-6842

PROJECT:

HARES HILL BRIDGE, CHESTER COUNTY, PA

SHEET NOTES:

NO.	DESCRIPTION	DATE	BY
1	INITIAL SUBMITTAL	5/4/05	

DESIGNED BY:	RJC AND HNM
DRAWN BY:	HNM
CHECKED BY:	RJC
SCALE:	VARIES
DATE:	5/18/05
PROJECT NO.:	AT149.1
SHEET TITLE:	

SHEET TITLE

SHEET NO.:

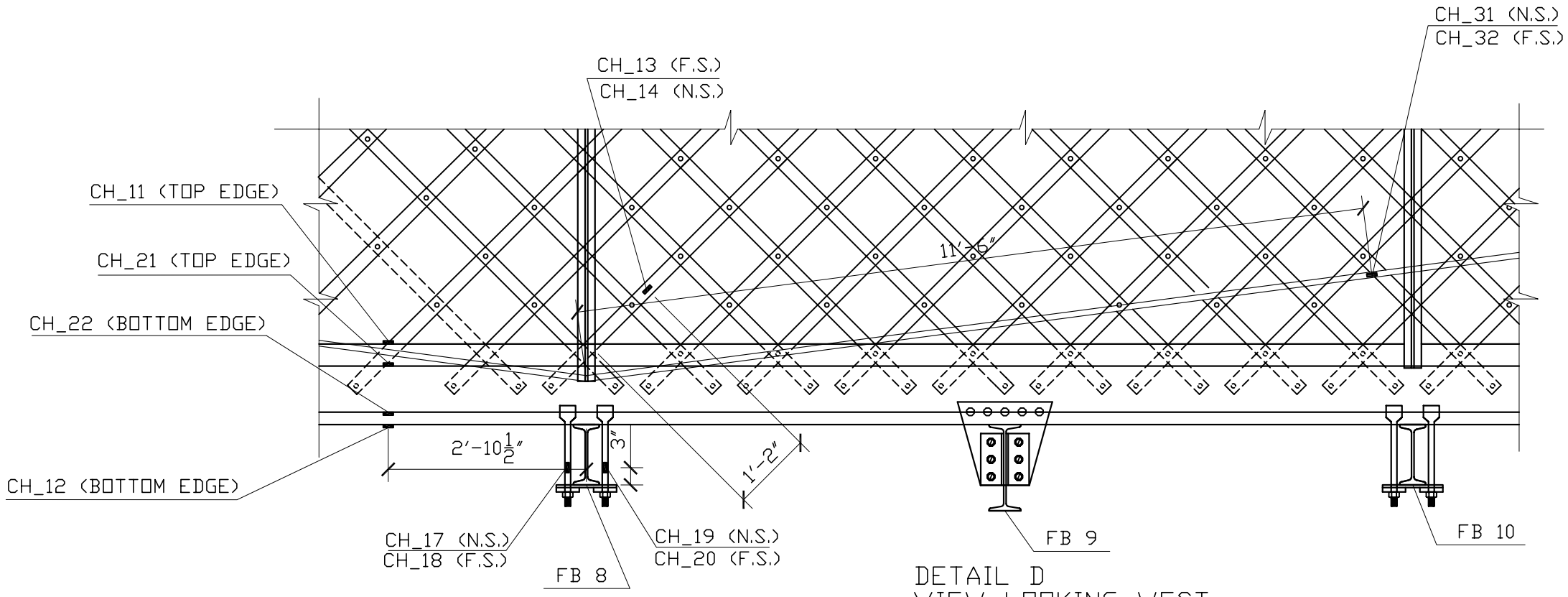

DETAIL D
VIEW LOOKING WEST
SCALE: 1/2' = 1'

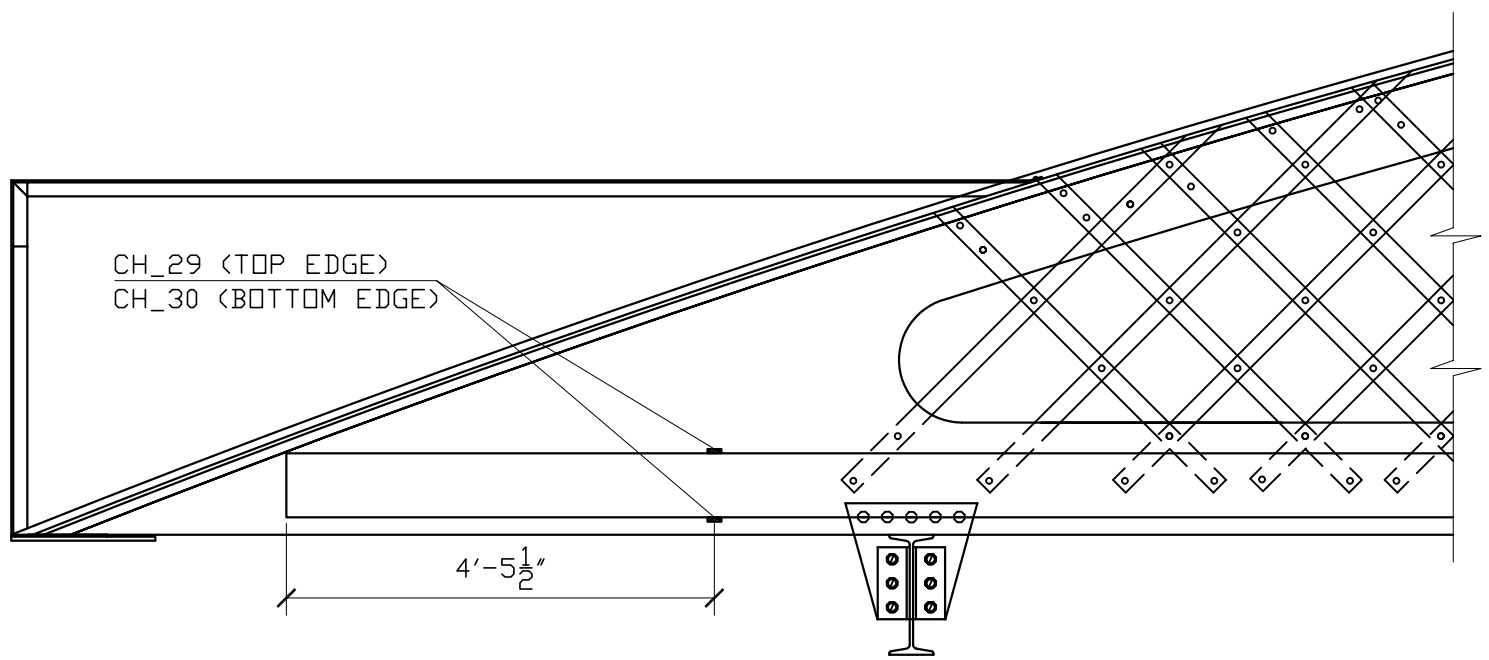

DETAIL E
VIEW LOOKING WEST
SCALE: 1/2" = 1'

ATLSS
117 ATLSS Drive
Lehigh University
Bethlehem, PA 18015
610-758-3535 FAX 610-758-6842

PROJECT:

HARES HILL BRIDGE, CHESTER COUNTY, PA

SHEET NOTES:

NO.	DESCRIPTION	DATE	BY
1	INITIAL SUBMITTAL	5/4/05	

DESIGNED BY:	RJC AND HNM
DRAWN BY:	HNM
CHECKED BY:	RJC
SCALE:	1/2" = 1'-0"
DATE:	5/18/05
PROJECT NO.:	AT149.1

SHEET TITLE:

SHEET TITLE

SHEET NO.:

Appendix B

Material Testing

B.0 Mechanical Properties Test Results

B.1 Tensile and Charpy V-notch Tests

Portion of materials were extracted from the web and flange of floobeam 1, web and flange of floorbeam 2, and the lower tie plate near the abutment. The materials were extracted using an electric saw. Half inch holes were drilled to assist in extracting the materials and to reduce the stress concentration located at the intersecting cuts.

From the extracted pieces, a total of seven tensile test specimens were machined from a portion of the flange of floorbeam 1, portion of the flange of floorbeam 2, and portion of the lower tie plate near the abutment. Specifically, two tensile specimens (1T1 and 1T2) were machine from the flange of floorbeam 1, which is made of structural steel, two tensile specimens (2T1 and 2T2) from the flange of floorbeam 2, which is made of wrought iron, and three tensile specimens (3T1, 3T2, and 3T3) from the lower tie plate near the south abutment, which is also made of wrought iron. The sampling and the testing was done in accordance with ASTM A370. In addition to the tensile test specimens machines from the portion of the extracted flange of floorbeam 1, three Charpy V-notch specimens were sampled and machined from the flange of the same extracted portion. Sampling and machining of the Cahrpy V-notch specimens was done in accordance with ASTM E23. Figure B.1 shows floorbeam 1 after the extraction of a small portion of the flange and the web. Detailed drawings of the size of the specimens and the location from which the specimens were machined can be found in Appendix C.

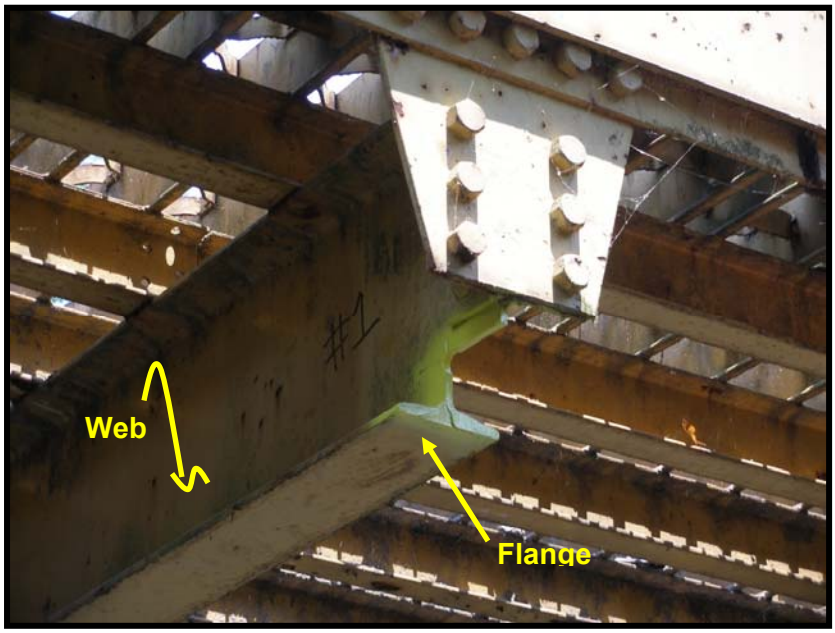

Figure B.1 - Floorbeam 1 after the extraction of a small portion of the flange and the web

The yield strength of the specimens machined from the flange of floorbeam 1 was measured to be 33.1 ksi in specimen 1T1 and 31.8 ksi in specimen 1T2. These values are typical of Gr. 33 (ASTM A7) structural steel shapes. The percent elongation in 2 inch

was measured to be 36.6% in specimen 1T1 and 35.9% in specimen 1T2, which exceeds the minimum of 23% specified by the specification.

In addition to the tensile tests, three Charpy V-notch specimens were sampled and machined from the same flange in accordance with ASTM E23, the Charpy V-notch tests were performed at the AASHTO Zone 2 test temperature (40^{o} F). Only one of the Charpy specimens satisfied the 15 ft-lb @ 40^{o} F toughness requirement. The CVN energy values in the three specimens were found to be 12.5 ft-lbs, 14.0 ft-lbs, and 15.0 ft-lbs, with an average of 13.7 ft-lbs.

The yield strength of the specimens machined from the flange of floorbeam 2 was measured to be 33.1 ksi in specimen 2T1 and 27.3 ksi in specimen 2T2. These values are typical of wrought iron. The percent elongation in 2 inch was measured to be 21.2% in specimen 2T1 and 26.2% in specimen 2T2. Although there is no minimum required value for percent elongation for wrought iron, the values measured would be considered a border line for the accepted minimum value for a typical structural steel.

The yield strength of the specimens machined from the lower tie plate near the abutment was measured to be 22.3 ksi in specimen 3T1, 31.1 ksi in specimen 3T2, and 31.4 in specimen 3T3. The low yield strength value measured in specimen 3T1 is not uncommon since the yield strength of wrought iron is highly dependent on the quantity and orientation of the non-metallic inclusions. The percent elongation in 2 inch was measured to be 7.5% in specimen 3T1 and 6.2% in specimen 3T2. The very low percent elongation value is also attributed to the quantity and oriantaion of the non-metailc inclusions present in the specimen. The measured percent elongation values are considered very low and well below what would be accepted for typical structural steel.

Location	Specimen Number	Yield Strength (ksi)	Tensile Strength (ksi)	Elongation (2") (%)	Area Reduction (%)	CVN Energy (ft-lbs @ 40 ^{o}F)
Flange of floorbeam 1	**1T1**	33.1.	64.4	36.6	52.1	12.5 14.0
	1T2	31.8	62.1	35.9	54.4	15.0 Avg. 13.7
Flange of floorbeam 2	**2T1**	33.1	54.7	21.2	23.4	23.4
	2T2	27.3	49.5	26.5	26.1	26.1
Lower tie plate near the south abutment	**3T1**	22.3	39.8	7.5	5.3	5.3
	3T2	31.1	38	N/A[1]	N/A[1]	N/A[1]
	3T3	31.4	39.5	6.2	5.1	5.1

Note:
1. Fracture occurred outside the gage length

Table B.1 – Summary of tensile test results of the flange material extracted from floorbeam 1, the flange material extracted from floorbeam 2, and from the lower tie plate near the abutment

B.2 Chemical Composition

The chemical analysis was conducted at Laboratory Testing Inc. of Hatfield, Pa. Results of the analysis from samples from the flange of floorbeam 1, the flange of floorbeam 2, and the lower tie plate near the abutment are reproduced and shown in Table B.2. The chemical compositions of the flange of floorbeam 1 (Specimen #1) were found to be in conformance to ASTM A7 and are acceptable. The chemical compositions of the flange of floorbeam 2 (Specimen #2) and the lower tie plate near the abutment (Specimen #3) were found to be typical of wrought iron.

Element	Specimen #1	Specimen #2	Specimen #3
Al	0.001%	-	-
C	0.21%	0.015%	0.005%
Cb	<0.001%	-	-
Cr	0.022%	-	-
Cu	0.27%	-	-
Mn	0.45%	0.045%	0.045%
Mo	0.009%	-	-
Ni	0.076%	-	-
P	0.01%	0.31%	0.17%
S	0.03%	0.027%	0.033%
Si	<0.01%	0.18%	0.19%
V	0.001%	-	-

Table B.2 – Summary of the chemical composition results of the flange material extracted from floorbeam 1 (Specimen #1), the flange material extracted from floorbeam 2 (Specimen #2), and from the lower tie plate near the abutment (Specimen #3)

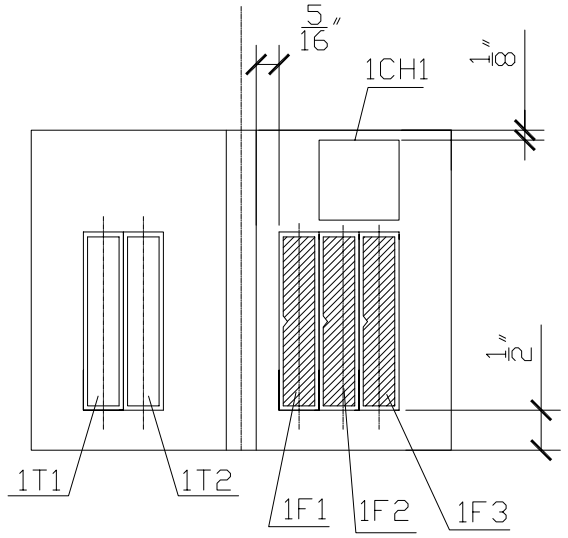

SPECIMEN #1 PLAN VIEW

SCALE: 5" = 1'

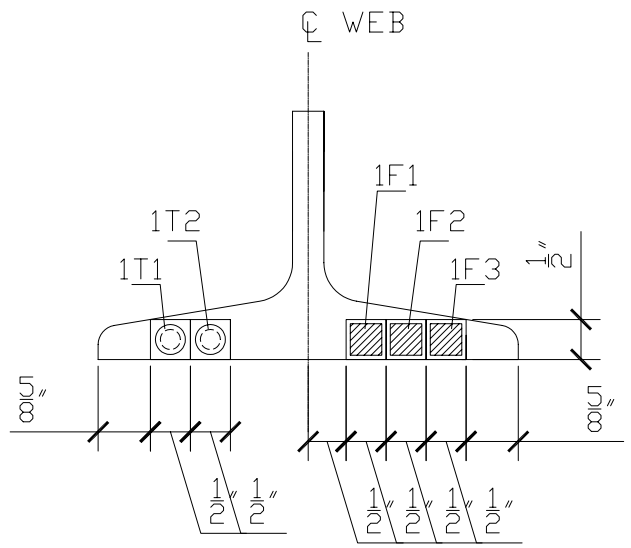

SPECIMEN #1 ELEVATION

SCALE: 5" = 1'

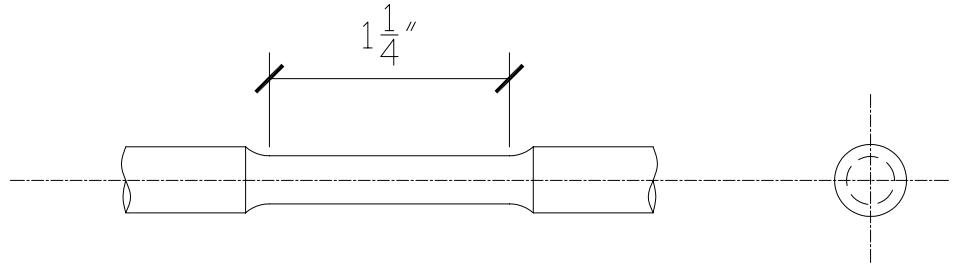

DETAIL A

ROUND TENSION TEST SPECIMEN (A370)

SCALE: 12" = 1'

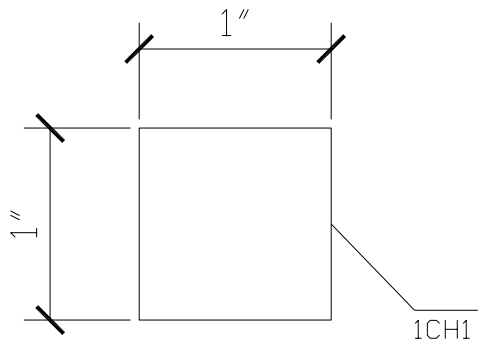

DETAIL B

CHEMICAL SPECIMEN (A572)

SCALE: 12" = 1'

NOTES (TENSILE TESTING):

1. SPECIMEN #1 IS MADE OF STRUCTURAL STEEL

2. TWO TENSION TEST SPECIMENS SHALL BE MACHINED FROM THE FLANGE OF SPECIMEN #1 AND SHALL BE MARKED AS 1T1 AND 1T2.

3. TENSILE SPECIMENS SHALL BE STANDARD ROUND 0.252 INCH TENSION TEST SPECIMEN PER ASTM A370 WITH DIAMETER AND THREAD SIZE OF 3/8-16 (SEE DETAIL A).

NOTES (CHEMICAL TESTING):

1. ONE CHEMICAL SPECIMEN SHALL BE MACHINED FROM THE FLANGE OF SPECIMEN #1 AND MARKED AS 1CH1 (SEE DETAIL B).

NOTES (CHARPY TESTING):

1. THREE CHARPY SPECIMENS SHALL BE MACHINED FROM THE FLANGE OF SPECIMEN #1 (FLANGE ON ONE SIDE OF THE WEB) AND SHALL BE MARKED AS 1F1, 1F2, AND 1F3

2. ALL CHARPY MACHINING SHALL BE PER ASTM E23.

ATLSS

ADVANCED TECHNOLOGY FOR LARGE STRUCTURAL SYSTEMS
117 ATLSS Drive
Lehigh University
Bethlehem, PA 18015
610-758-3535 FAX 610-758-6842

PROJECT:

HARES HILL ROAD BRIDGE

SHEET NOTES:

MATERIAL TESTING

NO.	DESCRIPTION	DATE	BY
1	INITIAL SUBMITTAL	7/6/05	HNM

DESIGNED BY:	HNM
DRAWN BY:	HNM
CHECKED BY:	EK
SCALE:	VARIES
DATE:	7/5/05
PROJECT NO.:	AT149.1
SHEET TITLE:	

MATERIAL TESTING SPECIMEN #1

SHEET NO.:

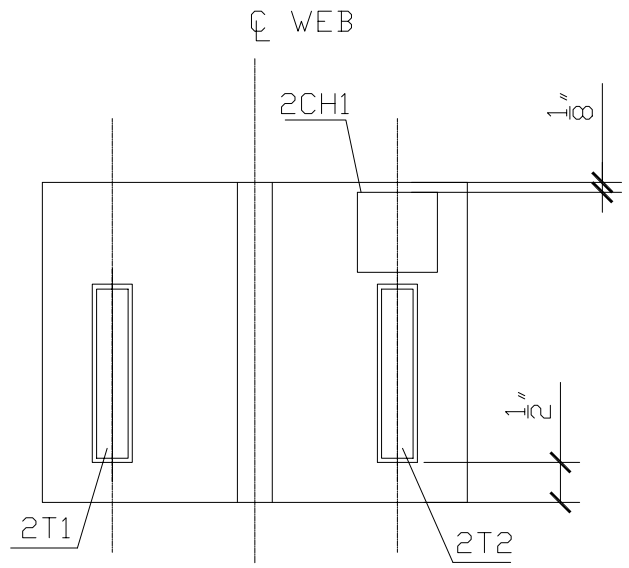

SPECIMEN #2 PLAN VIEW

SCALE: 5" = 1'

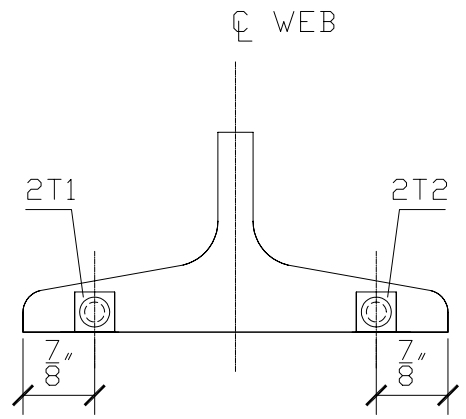

SPECIMEN #2 ELEVATION

SCALE: 5" = 1'

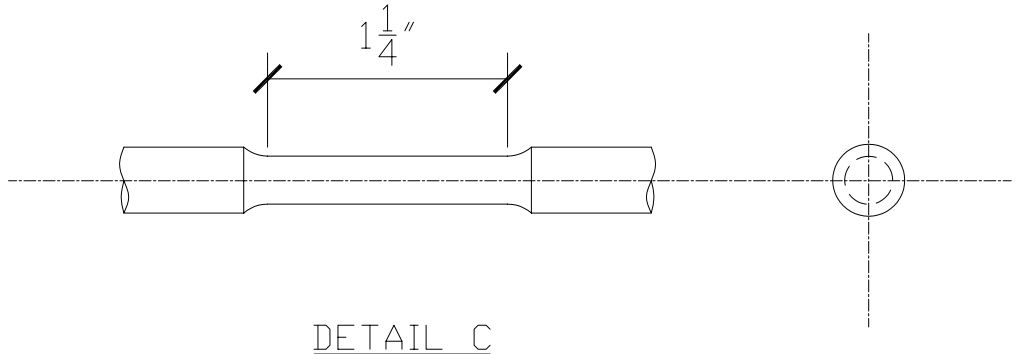

DETAIL C

ROUND TENSION TEST SPECIMEN (A370)

SCALE: 12" = 1'

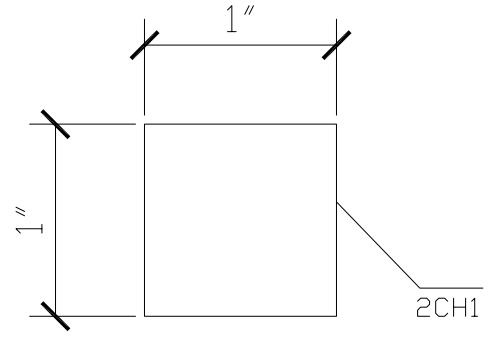

DETAIL D

CHEMICAL SPECIMEN (A572)

SCALE: 12" = 1'

NOTES (TENSILE TESTING):

1. SPECIMEN #2 IS MADE OF WROUGHT IRON STEEL.

2. TWO TENSION TEST SPECIMENS SHALL BE MACHINED FROM THE FLANGE OF SPECIMEN #2 (ONE SPECIMEN PER FLANGE ON EACH SIDE OF THE WEB) AND SHALL BE MARKED AS 2T1 AND 2T2.

3. TENSILE SPECIMENS SHALL BE STANDARD ROUND 0.252 INCH TENSION TEST SPECIMEN PER ASTM A370 WITH DIAMETER AND THREAD SIZE OF 3/8-16 (SEE DETAIL C).

NOTES (CHEMICAL TESTING):

1. ONE CHEMICAL SPECIMEN SHALL BE MACHINED FROM THE FLANGE OF SPECIMEN #2 AND MARKED AS 2CH1 (SEE DETAIL D).

ATLSS
ADVANCED TECHNOLOGY FOR LARGE STRUCTURAL SYSTEMS
117 ATLSS Drive
Lehigh University
Bethlehem, PA 18015
610-758-3535 FAX 610-758-6842

PROJECT:

HARES HILL ROAD BRIDGE

SHEET NOTES:

MATERIAL TESTING

NO.	DESCRIPTION	DATE	BY
1	INITIAL SUBMITTAL	7/6/05	HNM

DESIGNED BY:	HNM
DRAWN BY:	HNM
CHECKED BY:	EK
SCALE:	VARIES
DATE:	7/5/05
PROJECT NO.:	AT149.1
SHEET TITLE:	

MATERIAL TESTING SPECIMEN #2

SHEET NO.:

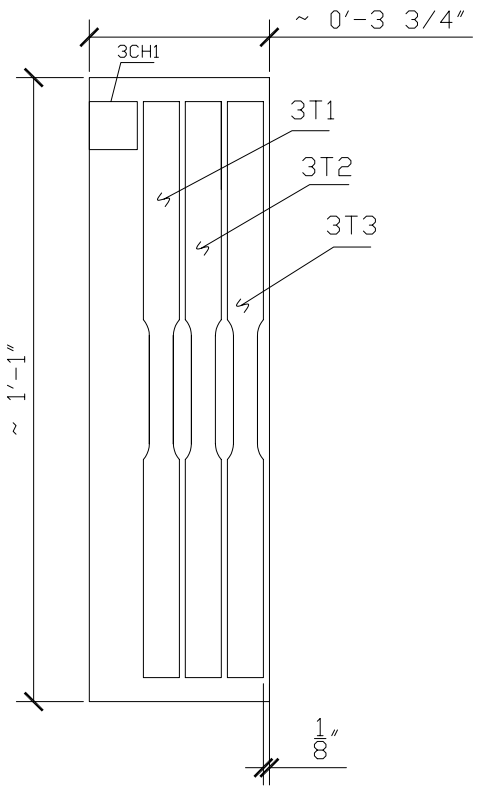

SPECIMEN #3
SCALE: 3" = 1'

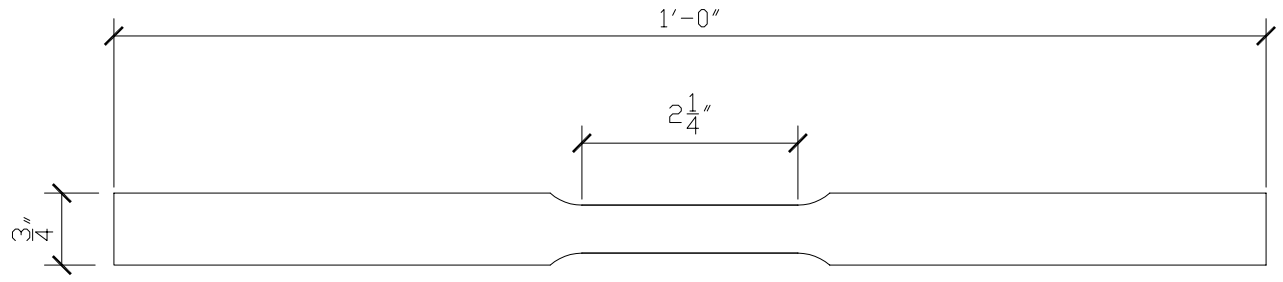

DETAIL E
TENSION TEST SPECIMEN (A370)
SCALE: 6" = 1'

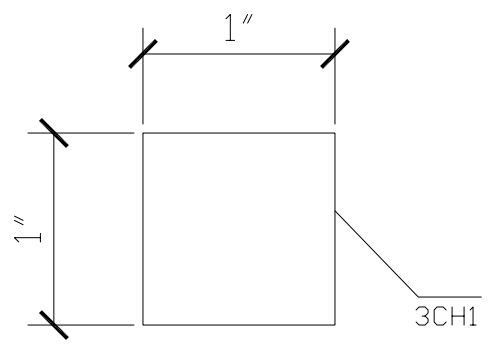

DETAIL F
CHEMICAL SPECIMEN (A572)
SCALE: 12" = 1'

NOTES (TENSILE TESTING):

1. SPECIMEN #3 IS MADE OF WROUGHT IRON STEEL.

2. THREE TENSION TEST SPECIMENS SHALL BE MACHINED FROM SPECIMEN #3 AND MARKED AS 3T1, 3T2, AND 3T3.

3. TENSILE SPECIMENS SHALL BE STANDARD SHEET-TYPE TENSILE SPECIMEN PER ASTM A370 (SEE DETAIL E).

NOTES (CHEMICAL TESTING):

1. ONE CHEMICAL SPECIMEN SHALL BE MACHINED FROM SPECIMEN #3 AND SHALL BE MARKED AS 3CH1 (SEE DETAIL F).

ATLSS
ADVANCED TECHNOLOGY FOR LARGE STRUCTURAL SYSTEMS
117 ATLSS Drive
Lehigh University
Bethlehem, PA 18015
610-758-3535 FAX 610-758-6842

PROJECT:

HARES HILL ROAD BRIDGE

SHEET NOTES:

MATERIAL TESTING

NO.	DESCRIPTION	DATE	BY
1	INITIAL SUBMITTAL	7/6/05	HNM

DESIGNED BY:	HNM
DRAWN BY:	HNM
CHECKED BY:	EK
SCALE:	varies
DATE:	7/5/05
PROJECT NO.:	AT149.1
SHEET TITLE:	

MATERAIL TESTING SPECIMEN #3

SHEET NO.: